J. Fluid Mech. (2003), *vol.* 484, *pp.* 85–111.

DOI: 10.1017/S002211200300418X Printed in the United Kingdom

Near-contact electrophoretic motion of a sphere parallel to a planar wall

By E. YARIV AND H. BRENNER

Department of Chemical Engineering, Massachusetts Institute of Technology, Cambridge, MA 02139, USA

(Received 24 April 2002 and in revised form 1 December 2002)

The electrophoretic motion of a sphere resulting from an applied electric field directed parallel to a nearby plane wall is analysed for the case of a small sphere–wall gap width. The thin-Debye-layer approximation is employed. Using matched asymptotic expansions, the fluid domain is separated into an 'inner' (gap-scaled) region, wherein the electric field and velocity gradients are large, and an 'outer' (sphere-scaled) region, wherein field variations are moderate. Asymptotic expressions for the force and torque acting on the sphere are obtained using a reciprocal theorem, thereby avoiding the need to explicitly solve the pertinent Stokes equations. These expressions, as well as the sphere's electrophoretic mobility, become unbounded for near-contact separations. The present asymptotic solution complements existing 'exact' bipolar-coordinate eigenfunction expansions, which are numerically suitable only for $O(1)$ gap thicknesses.

1. Introduction

The problem of electrophoretic motion near boundaries possesses practical significance for a diverse class of applications involving bounded electrokinetic flows, ranging from traditional gel electrophoresis to those occurring in microfluidic devices. The Helmholtz–Smoluchowski mobility approximation fails to provide an appropriate model for these applications, as it does not capture any wall effects. Such effects may be substantial in the case of particles moving through narrow channels, since the electrophoretic mobility may vary significantly as the particles approach the walls (Keh & Chen 1989). Moreover, while simplified mobility models may suffice to describe the mean particle motion, more rigorous analysis is required to understand the nonlinear Taylor dispersion phenomena accompanying these transport processes. The virtual absence of dispersion during processes involving 'point-size' particles (which do not experience wall effects) is one of the principal reasons why electrokinetic separation is preferred over alternative methods, such as hydrodynamic chromatography.

Electrokinetic flows represent a balance between animating electrical body forces, acting on electrically non-neutral fluid elements, and retarding viscous stresses. The regions of non-neutrality, known as Debye double layers, form in proximity to charged surfaces (such as colloidal particle boundaries). The system of equations governing the flow and transport processes occurring within these layers is coupled as well as highly nonlinear (Russel, Saville & Schowalter 1989). As typical applied electric fields are relatively weak compared with those existing within the layer, it is common to linearize these equations about an equilibrium Debye-layer structure, with the leading-order perturbations being proportional to the applied field (O'Brien & White 1978). This procedure yields a linear relation between the externally applied field and resulting particle velocity, leading thereby to the concept of electrophoretic mobility.

A further simplification (O'Brien & Hunter 1981; O'Brien 1983) is made possible based upon the relatively small thickness of the layer. Indeed, even in the case of miniaturized microfluidic devices (Stone & Kim 2001), the Debye-layer width, say κ^{-1}, is usually small relative to the pertinent 'macroscale' length scales (e.g. channel width or solute particle dimension). The flow domain is therefore conceptually separated into two regions: the first consists of thin Debye layers surrounding the various surfaces in contact with the electrolyte, whereas the second region consists of the electrically neutral bulk fluid domain. Integration of the transport equations within the Debye layers in a direction normal to the charged surfaces provides boundary conditions to be imposed at the bulk-scale level of description (wherein these layers appear as singular surfaces). Hence, the pertinent bulk flows are governed by the conventional Stokes equations (with no electrical body forces), albeit with 'slip' conditions imposed at the charged boundaries. This slip reflects a finite velocity jump across the Debye layer, whose magnitude is proportional to the local value of the macroscale electric field at the boundary (Keh & Anderson 1985). This field, in turn, is derived from an electric potential. The latter satisfies Laplace's equation within the bulk fluid domain, subject to Neumann-type conditions on the boundaries.

Many practical electrokinetic processes involve solute transport occurring in dilute dispersions, for which circumstances it suffices to restrict attention to boundary effects upon the motion of a single particle. Using the thin Debye-layer formalism described above, Morrison (1970) demonstrated that such a particle would translate with the Smoluchowski velocity in the absence of boundaries, and would not rotate. These conclusions do not generally hold in the presence of solid walls (or other particles). However, within the thin-Debye-layer formalism, such boundaries do not pose significant computational difficulties, given the ubiquity of the Stokes and Laplace equations.

The simplest wall effect model entails a sphere moving under the influence of an applied electric field directed parallel to a nearby plane wall. This problem was originally analysed for large sphere–wall separations using successive reflections (Keh & Anderson 1985). As would be expected, the presence of the wall acts as to reduce the particle velocity (compared with the Smoluchowski value appropriate for a particle in an unbounded fluid). Subsequently, an exact solution to this problem was furnished by Keh & Chen (1989) using bipolar coordinates to evaluate the electric potential in the fluid, as well as to calculate the resulting fluid velocity field. In this coordinate system, the electric potentials, together with the velocity and pressure fields, appear as eigenfunction expansion series, the respective coefficients of which were evaluated by truncating an infinite algebraic system of equations. For large particle–wall separations, the results of Keh & Chen predicted a reduction in electrophoretic mobility, in agreement with the reflection expressions provided by Keh & Anderson (1985). However, decreasing separations reverse this trend, whence the particle velocity is enhanced with a diminishing sphere–wall gap distance. Moreover, as this clearance vanishes, the force and torque exerted on the sphere (and, as a result, its electrophoretic mobility) all become unbounded. (As bipolar-coordinate expressions invariably converge poorly for separations approaching contact, Keh & Chen were apparently unable to obtain precise results for separations smaller than about half a percent of the sphere radius.) This interesting phenomenon is qualitatively different from that for comparable particle motion throughout an electrolyte-free liquid under the influence of an external field, wherein the logarithmic divergence of the drag forces (Happel & Brenner 1965) results in diminishing particle velocities at near-contact separations.

The analysis which follows furnishes asymptotic expressions for the force and torque on the sphere when the gap is small compared with the sphere's radius. This complements the eigenfunction expansions of Keh & Chen (1989), in the same sense as the small-gap analysis of O'Neill & Stewartson (1967) complements the creeping-flow bipolar-coordinate solution of O'Neill (1964) for the problem of a sphere translating parallel to a wall (in the absence of electrokinetic effects). As such, this work may be of interest in various applications, as accurate mobility models for small separation distances are important for various fields, such as electrophoretic aggregation (Zeng, Zinchenko & Davis 1999) and crystallization on an electrode surface (Böhmer 1996). Indeed, the poor convergence of bipolar-coordinate expressions for separations approaching contact has led to attempts to improve the convergence of such expressions (Zeng *et al.* 1999).

In the pioneering small-gap analysis of O'Neill & Stewartson (1967) the fluid domain was separated into two regions: an inner, gap-scaled, region, in the neighbourhood of the closest separation between the sphere and the wall; and an outer region (wherein, to leading order, the sphere appears to be touching the wall) consisting of the remaining flow domain. The flow problem in the outer region was solved using tangent-sphere coordinates, with the velocity and pressure fields eventually expressed as Hankel transforms. These expressions become singular at the 'contact' point. Within the inner region, velocity gradients and pressures are large in magnitude, and the solution possesses a lubrication-type structure. A similar analysis was carried out by Cooley & O'Neill (1968) for the case of a sphere rotating about an axis parallel to a nearby wall.

O'Neill & Stewartson's solution scheme has become a standard asymptotic technique for resolving other physical problems involving small particle–wall separations (e.g. Hu & Joseph 1999 for the case of a non-Newtonian fluid). As a matter of fact, the near-contact geometry has also been employed in electrokinetic analysis, albeit for a different physical problem involving electrokinetic lift (see e.g. Warszyński, Wu & van de Ven 1998, who analysed the case of an infinite cylinder in the proximity of a wall). However, such electroviscous forces are usually negligible during electrophoresis, at least when the Debye layers are thin (Cox 1997). As such, these analyses are not directly pertinent to the present investigation.

The first small-gap solution of Laplace's equation subject to Neumann-type boundary conditions (Jeffrey & Chen 1977) was carried out for the axisymmetric case (wherein the applied field acts perpendicular to the wall). The comparable asymmetrical case of a field acting parallel to the plane is more difficult to solve. The outer solution thereof was obtained by Latta & Hess (1973) in the context of irrotational flows, using inversion methods. The respective inner solution was obtained by Solomentsev, Velegol & Anderson (1997) to terms of leading order in the dimensionless gap width.

Once the electric potential solution is obtained, the boundary 'slip' conditions to be imposed upon the fluid velocity field at the sphere and wall surfaces may be considered as 'known'. Owing to the linearity of the resulting Stokes-flow problem, it proves convenient to decompose the requisite boundary-value problem posed at the sphere and wall surfaces – together with their respective contributions to the total force and torque acting on the sphere – into four distinct parts. The first two are respectively associated with the translation and rotation of a sphere near a plane wall in the absence of slip on both surfaces, for which appropriate asymptotic approximations already exist (O'Neill & Stewartson 1967; Cooley & O'Neill 1968). The third and fourth contributions, pertaining to electrokinetic slip, depend upon the electric field distribution at the sphere surface.

Given the slip conditions on the sphere (in terms of the above-mentioned electric field), it is possible in principle to evaluate the resulting Stokes flow and hence the consequent tractions on the sphere. However, the requisite algebra turns out to be forbidding. Instead, we employ a reciprocal theorem (Brenner 1964), which reduces the evaluation of the force (torque) on the sphere to a straightforward quadrature requiring knowledge only of the classical (electrolyte-free) stress field resulting from movement of a translating (rotating) sphere in proximity to the wall in a fluid otherwise at rest. This procedure furnishes the desired expressions for the force and torque. The dominant terms in these expressions, which diverge as a negative irrational power of the gap width, are explicitly evaluated based upon knowledge of the electric potential and flow-field distribution over the inner portion of the sphere's surface. Comparison of this divergent behaviour with the 'exact' bipolar-coordinate results confirms excellent agreement of the two schemes. The $O(1)$ coefficients appearing in these expressions, which depend upon the fields in the outer region, are evaluated using a 'patching' procedure with this 'exact' solution, in a manner similar to that employed by Goldman, Cox & Brenner (1967*a*).

A unique feature of the present analysis is that the actual Stokes equations are never explicitly solved during the course of obtaining the force and torque (using, instead, the reciprocal theorem). This feature renders the present perturbation scheme attractive with regard to resolving other classes of problems involving particle–wall flows in which the velocity field is coupled (through boundary conditions on the particle surface) to another field satisfying Laplace's equation. A typical case would be that of the thermophoretic motion of a drop parallel to a plane wall (cf. Loewenberg & Davis 1993).

The paper is organized as follows. The overall problem formulation, governing the electric potential and flow fields, as well as the decomposition of the flow field into four distinct parts, is described in § 2 for arbitrary sphere–wall separations. Detailed expressions for the electric field in both the outer and inner regions are provided in § 3 for the case of small gap widths. Evaluations of the third and fourth contributions to the force and torque are respectively given in §§ 4 and 5. Section 6 summarizes and discusses the results obtained.

2. Formulation

Consider a spherical colloidal particle moving within an electrolyte solution bounded by a stationary plane wall $\mathscr{W}$ under the influence of an applied uniform electric field $\boldsymbol{E}_\infty$ acting parallel to the plane. Both the sphere and plane are assumed to be non-conducting and to each possess uniform surface charge densities, with respective zeta potentials ζ_p and ζ_w. The sphere's radius is a and the closest distance of its surface from the wall is $a\delta$ (see figure 1). We employ Cartesian coordinates (ax, ay, az) with origin on the wall, in which the x-direction lies along the direction of $\boldsymbol{E}_\infty$, as well as cylindrical polar coordinates $(a\rho, \psi, az)$ having the same origin. The z-axis, which lies normal to $\mathscr{W}$, passes through the sphere centre O, whose Cartesian coordinates are $[0, 0, a(1+\delta)]$.

In the limit of small Debye-layer thickness, the respective matching conditions imposed upon the various fields in the transition region between the Debye layer

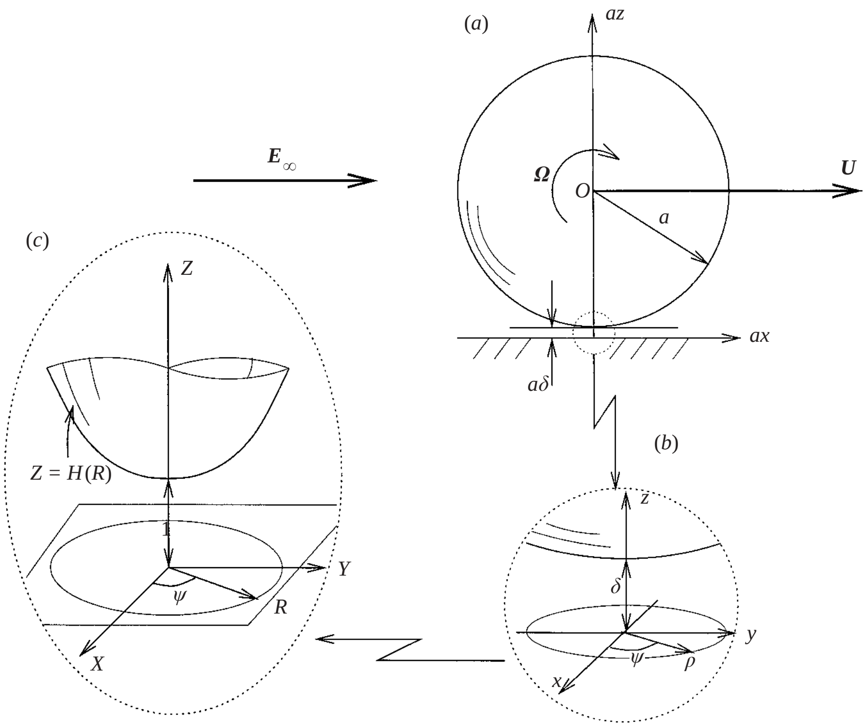

FIGURE 1. Particle–wall geometry: (*a*) particle scale; (*b*) gap-scaled region; (*c*) strained gap region.

and the 'bulk' fluid may be utilized as bulk-field boundary conditions at the various surfaces in contact with the fluid (O'Brien 1983; Keh & Anderson 1985). The first is that the normal component of the electric field vanishes,

$$\boldsymbol{n} \cdot \nabla \Phi = 0, \tag{2.1}$$

where $\Phi(\boldsymbol{x})$ is the electric potential at the point $\boldsymbol{x}$, and $\boldsymbol{n}$ the unit vector normal to the boundary (pointing into the fluid). The second condition is that the fluid 'slips' on the surfaces at a velocity $(\varepsilon\zeta/\mu)\nabla\Phi$, where ε and μ are, respectively, the dielectric permittivity and viscosity of the fluid. For a sphere whose centre moves at velocity $\boldsymbol{U}$ and which rotates at an angular velocity $\boldsymbol{\Omega}$, the fluid velocity on the sphere's surface $\mathscr{P}$ is thus given by

$$\boldsymbol{v} = \frac{\varepsilon\zeta_p}{\mu}\nabla\Phi + \boldsymbol{U} + a\boldsymbol{\Omega} \times \boldsymbol{n}. \tag{2.2}$$

As the bulk region outside of the Debye layer is electrically neutral, the Poisson equation governing Φ degenerates to the Laplace equation, and electrical body forces are absent from the Navier–Stokes equations. Far from the sphere, $\Phi \sim -E_\infty a x$. Although the velocity field is coupled to the electrostatic field through the boundary condition (2.2), the electrostatic problem governing Φ may be solved independently.

In non-dimensionalization of the pertinent variables, we normalize length variables with a, velocities with the characteristic electrophoretic velocity, $\mathscr{U} = \varepsilon\zeta_p E_\infty/\mu$, angular velocities with $\mathscr{U}/a$, stresses with $\mu\mathscr{U}/a$, and the electric potential with $E_\infty a$. The Neumann-type boundary-value problem governing Φ consists of: (i) Laplace's equation in the fluid domain,

$$\nabla^2 \Phi = 0; \tag{2.3}$$

(ii) the boundary conditions on the sphere and wall,

$$\boldsymbol{n} \cdot \nabla \Phi = 0 \quad \text{on} \quad \mathscr{P} \cup \mathscr{W}; \tag{2.4}$$

and (iii) the far-field condition,

$$\Phi \to \Phi_\infty \equiv -x \quad \text{as} \quad |\boldsymbol{x}| \to \infty. \tag{2.5}$$

For typical scenarios, fluid inertia forces are negligible and the creeping-flow equations are applicable (Stone & Kim 2001). The problem governing the flow field consists of: (i) the continuity equation,

$$\nabla \cdot \boldsymbol{v} = 0; \tag{2.6}$$

(ii) the Stokes equations,

$$\nabla^2 \boldsymbol{v} = \nabla p; \tag{2.7}$$

(iii) the boundary condition on the sphere,

$$\boldsymbol{v} = \nabla \Phi + \boldsymbol{U} + \boldsymbol{\Omega} \times \boldsymbol{n} \quad \text{on} \quad \mathscr{P}; \tag{2.8}$$

(iv) the boundary condition on the wall,

$$\boldsymbol{v} = \gamma \nabla \Phi \quad \text{on} \quad \mathscr{W}; \tag{2.9}$$

and (v) the far-field condition,

$$\boldsymbol{v} \to \gamma \nabla \Phi_\infty \quad \text{as} \quad |\boldsymbol{x}| \to \infty. \tag{2.10}$$

In the above, $\gamma = \zeta_w/\zeta_p$, and $\gamma \nabla \Phi_\infty$ $(= -\gamma \boldsymbol{e}_x)$ is the uniform electro-osmotic velocity far from the sphere. Once the velocity and pressure fields are obtained, the hydrodynamic stress field $\boldsymbol{\pi}$ may be calculated from the expression

$$\boldsymbol{\pi} = -p\boldsymbol{I} + \left[\nabla \boldsymbol{v} + (\nabla \boldsymbol{v})^\dagger\right], \tag{2.11}$$

where $\boldsymbol{I}$ is the dyadic idemfactor. As Φ may be determined (up to an irrelevant additive constant) by equations (2.3)–(2.5), the velocity field is defined well by (2.6)–(2.10). In principle, the present linear problem can be solved to obtain the electric potential Φ, fluid velocity $\boldsymbol{v}$, and pressure field p.

Formally speaking, the force and torque acting on the sphere may be expressed as surface integrals involving the stress field (incorporating electric Maxwell stresses) evaluated at the sphere's actual boundary (that is, at the inner edge of the Debye layer). However, since the stress field is symmetric and divergence-free throughout the entire fluid domain (and, in particular, within the Debye layer), these integrals may be performed at the outer edge of the layer (namely over $\mathscr{P}$). In general, the Maxwell stresses do not vanish in the bulk region. However, since these stresses are quadratic in the electric field, their contribution is negligible in the context of the present linear electrophoretic analysis. Integration of the hydrodynamic stress field (2.11) yields the hydrodynamic force (normalized with $6\pi\mu\mathscr{U}a$),

$$\boldsymbol{F} = \frac{1}{6\pi} \oint_{\mathscr{P}} \mathrm{d}S\, \boldsymbol{n} \cdot \boldsymbol{\pi}, \tag{2.12}$$

and torque (normalized with $8\pi\mu\mathscr{U}a^2$) about the sphere centre, $\boldsymbol{x}_O$,

$$\boldsymbol{T} = \frac{1}{8\pi} \oint_{\mathscr{P}} \mathrm{d}S\, (\boldsymbol{x} - \boldsymbol{x}_O) \times (\boldsymbol{n} \cdot \boldsymbol{\pi}), \tag{2.13}$$

exerted by the fluid on the sphere. Both $\boldsymbol{F}$ and $\boldsymbol{T}$ are obviously linear in each of the parameters $\boldsymbol{E}_\infty(=\boldsymbol{e}_x)$, $\boldsymbol{U}$ and $\boldsymbol{\Omega}$. For a force- and couple-free particle, equating these two to zero yields the sphere's velocities, $\boldsymbol{U}$ and $\boldsymbol{\Omega}$, as linear functions of $\boldsymbol{E}_\infty$. Since $\boldsymbol{e}_z$ the only space-fixed geometrically specified vector characterizing the problem, it is clear that the *vector* $\boldsymbol{U}$ is proportional to $\boldsymbol{E}_\infty$, whereas the *pseudo-vector* $\boldsymbol{\Omega}$ is proportional to $\boldsymbol{e}_z \times \boldsymbol{E}_\infty$. With $\boldsymbol{E}_\infty$ pointing in the x-direction, we conclude that $\boldsymbol{U} = U\boldsymbol{e}_x$ and $\boldsymbol{\Omega} = \Omega\boldsymbol{e}_y$ (the latter result is also deducible from symmetry considerations).

Owing to the linearity of the flow problem, it is convenient to decompose the flow field ($\boldsymbol{v}$, p) into four distinct contributions, labelled (a)–(d), each satisfying the flow equations (2.6)–(2.7) and the following boundary conditions:

$$\begin{array}{lcccc} & \text{(a)} & \text{(b)} & \text{(c)} & \text{(d)} \\ \text{on } \mathscr{P}: & \boldsymbol{v} = \boldsymbol{U} & \boldsymbol{v} = \boldsymbol{\Omega} \times \boldsymbol{n} & \boldsymbol{v} = (1-\gamma)\nabla\Phi & \boldsymbol{v} = \gamma\nabla\Phi \\ \text{on } \mathscr{W}: & \boldsymbol{v} = \boldsymbol{0} & \boldsymbol{v} = \boldsymbol{0} & \boldsymbol{v} = \boldsymbol{0} & \boldsymbol{v} = \gamma\nabla\Phi \\ \text{as } |\boldsymbol{x}| \to \infty: & \boldsymbol{v} \to \boldsymbol{0} & \boldsymbol{v} \to \boldsymbol{0} & \boldsymbol{v} \to \boldsymbol{0} & \boldsymbol{v} \to \gamma\nabla\Phi_\infty \end{array}$$

The total hydrodynamic force (torque) acting on the particle consists of the sum of the respective forces (torques) resulting from the separate motions (a)–(d). In terms of the resulting forces and torques, problem (a) is equivalent to that of a non-rotating sphere translating with a velocity $\boldsymbol{U}$ through an otherwise quiescent fluid, with no-slip on both the sphere and the wall. Likewise, problem (b) is equivalent to that of a non-translating sphere rotating about an axis through its centre with an angular velocity $\boldsymbol{\Omega}$ in an otherwise quiescent fluid, with no slip on both the sphere and the wall. Problems (c) and (d) reflect the electrokinetic portions of the overall flow problem posed.

The foregoing formulation applies for arbitrary sphere–wall separation distances. In what follows, we focus on the small gap limit, $\delta \ll 1$. Asymptotic solutions for small gap widths already exist for both the Laplace equation (Jeffrey & Chen 1977; Jeffrey 1978; Solomentsev *et al.* 1997) and the creeping-flow equations (O'Neill & Stewartson 1967; Cooley & O'Neill 1968) in the context of several physical problems. In obtaining these solutions it was observed that regular perturbations of the pertinent fields in powers of δ may become singular in the vicinity of the gap, where $|\boldsymbol{x}| \to 0$. Hence, such regular perturbation fields constitute *bona fide* solutions only in the outer region. The respective inner solutions (within the gap) of these equations have been obtained by the above-cited authors via an appropriate scaling of the coordinates. Using this asymptotic matching method, the respective hydrodynamic forces and torques corresponding to problems (a) and (b) have already been obtained (O'Neill & Stewartson 1967; Cooley & O'Neill 1968). In the present work we need therefore only solve problems (c) and (d). A preliminary step towards these solution is the evaluation of the electric potential. This is established in the next section.

3. The electric potential

3.1. *Outer solution*

In terms of the polar cylindrical coordinates, the surface of the sphere is given by the equation

$$(z - 1 - \delta)^2 + \rho^2 = 1. \tag{3.1}$$

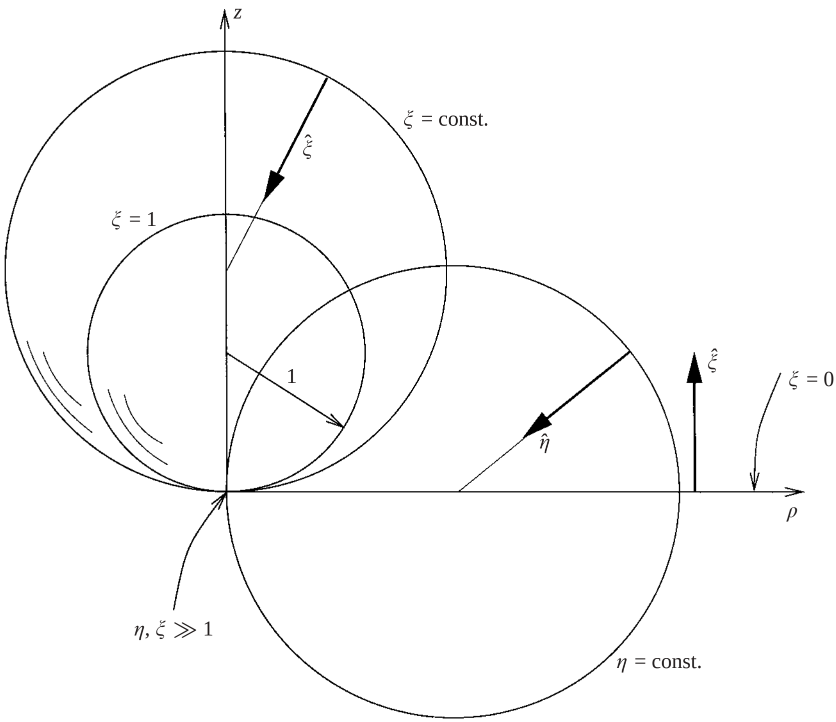

FIGURE 2. Tangent-sphere coordinate system: meridian plane view.

To leading order in δ, this surface is tangent to the wall. Hence, it is convenient to employ tangent-sphere coordinates, (ξ, η, ψ), defined as (Jeffrey 1978)

$$\rho = \frac{2\eta}{(\xi^2 + \eta^2)}, \qquad z = \frac{2\xi}{(\xi^2 + \eta^2)}, \tag{3.2}$$

in which the surface ξ = const. constitutes a sphere centred about the point $(0, 0, 1/\xi)$ and tangent to the plane $z = 0$ (see figure 2). In terms of these coordinates the wall is located at $\xi = 0$, whereas the sphere surface $\mathscr{P}$ is given by the equation

$$\xi \sim 1 + \delta \frac{\eta^2 - 1}{2} + O(\delta^2), \tag{3.3}$$

which, in the limit $\delta \to 0$, corresponds to the surface $\xi = 1$.

It is convenient to write $\Phi = \Phi_\infty + \varphi$, wherein $\Phi_\infty = -x$ is the potential far from the sphere. In the present small-δ analysis we need only evaluate the leading-order approximation to φ, say $\varphi^{(0)}$. In terms of the tangent-sphere coordinates, $\varphi^{(0)}$ satisfies the following boundary conditions: (i) on the sphere surface,

$$\frac{\partial \varphi^{(0)}}{\partial \xi} = -4 \frac{\eta}{(\eta^2 + 1)^2} \cos\psi \quad \text{at} \quad \xi = 1; \tag{3.4}$$

(ii) on the wall,

$$\frac{\partial \varphi^{(0)}}{\partial \xi} = 0 \quad \text{at} \quad \xi = 0; \tag{3.5}$$

and (iii) in the far field,

$$\varphi^{(0)} \to 0 \quad \text{for} \quad \xi, \eta \to 0. \tag{3.6}$$

Laplace's equation can be solved in tangent-sphere coordinates using Hankel transforms (Jeffrey 1978). Explicitly, the most general harmonic function which matches the azimuthal dependence of (3.4), satisfies the symmetry condition (3.5), and attenuates at infinity is (Moon & Spencer 1988)

$$\varphi^{(0)} = (\xi^2 + \eta^2)^{1/2} M(\xi, \eta) \cos\psi, \tag{3.7}$$

wherein

$$M(\xi, \eta) = \int_0^\infty sA(s) \cosh(\xi s)\, J_1(\eta s)\, \mathrm{d}s. \tag{3.8}$$

The function $A(s)$ is evaluated using the non-homogeneous boundary condition (3.4), which requires that

$$(\eta^2 + 1)\frac{\partial M}{\partial \xi} + M = -\frac{4\eta}{(\eta^2 + 1)^{3/2}} \quad \text{at} \quad \xi = 1. \tag{3.9}$$

Application of the Hankel transform of order one

$$\mathscr{H}_1\{f(s); s \longmapsto \eta\} = \int_0^\infty sf(s)\, J_1(\eta s)\, \mathrm{d}s, \tag{3.10}$$

in conjunction with the pair of relations (Sneddon 1972)

$$\mathscr{H}_1\{\eta^2 f(\eta); \eta \longmapsto s\} = -\left(\frac{\partial^2}{\partial s^2} + \frac{\partial}{\partial s} - \frac{1}{s^2}\right)\mathscr{H}_1\{f(\eta); \eta \longmapsto s\}, \tag{3.11}$$

$$\mathscr{H}_1\left\{\frac{\eta}{(\eta^2 + 1)^{3/2}}; \eta \longmapsto s\right\} = \mathrm{e}^{-s}, \tag{3.12}$$

yields the following differential equation governing $G(s) = sA(s)\sinh s$:

$$s^2 G'' + sG' - (1 + s^2 + s\coth s)G = 4s^2 \mathrm{e}^{-s}. \tag{3.13}$$

Once G is evaluated, M may be obtained by effecting the quadrature,

$$M = \int_0^\infty \frac{G(s)}{\sinh s} \cosh \xi s\, J_1(\eta s)\, \mathrm{d}s. \tag{3.14}$$

The problem governing $\varphi^{(0)}$ does not provide any boundary conditions to impose upon $G(s)$. However, in order that the integral (3.14) be convergent it is required that $G(s) \sim o(s^{-1})$ for $s \ll 1$, and that $G(s) \sim o(s)$ for $s \gg 1$. Near the regular singular point $s = 0$, one homogeneous solution is $G_1(s) = s^{\sqrt{2}}[1 + \frac{1}{3}(\sqrt{2}-1)s^2 + O(s^4)]$, whereas the other solution, $\sim s^{-\sqrt{2}}$, is non-integrable. The particular solution near that point is $G_{\mathrm{p}}(s) = 2s^2 - \frac{4}{7}s^3 + O(s^4)$. Consequently, $G(s) \sim Cs^{\sqrt{2}}$ for $s \ll 1$. Near the irregular singular point $s = \infty$, one homogeneous solution is e^{-s}/s, whereas the particular solution is $s\mathrm{e}^{-s}$. These solutions are exact up to exponentially small errors. The other homogeneous solution, $\sim \mathrm{e}^{s}$, is rejected since it leads to a divergent integral. Consequently, $G(s) \sim s\mathrm{e}^{-s}$ for $s \gg 1$. Equation (3.13) was integrated numerically twice: In the first integration, the expansion $G_1(s)$ was used for the starting (small) value of s; in the second integration, in which the right-hand-side of (3.13) was set to zero, the expansion $G_{\mathrm{p}}(s)$ was used. The coefficient C that made the linear combination of these two solutions $\sim s\mathrm{e}^{-s}$ for large s was chosen, yielding $C = -1.79119$. The above are essentially the results obtained by the inversion-method analysis of Latta & Hess (1973) in the context of irrotational flow.†

The behaviour of $\varphi^{(0)}$ at infinity, where both η and ξ are small, is dominated by the contribution to the integral representation (3.14) arising from the region $s \sim O(\xi^{-1})$. Use of the asymptotic form of $G(s)$ for large arguments yields, in terms of the integration variable $t = \xi s$,

$$M \sim \frac{2}{\xi^2} \int_0^\infty t\, J_1(\eta t/\xi)\, \mathrm{e}^{-2t/\xi} \cosh t \,\mathrm{d}t. \tag{3.15}$$

Evaluation (Sneddon 1972) of the latter integral yields

$$\varphi^{(0)} \sim \tfrac{1}{4}\eta(\eta^2 + \xi^2)^{1/2} \cos\psi, \tag{3.16}$$

or, in terms of cylindrical polar coordinates,

$$\varphi^{(0)} \sim \frac{\rho}{(\rho^2 + z^2)^{3/2}} \cos\psi, \tag{3.17}$$

corresponding to a dipole oriented in the negative x-direction.

The behaviour of $\varphi^{(0)}$ near the gap, where $\eta \gg 1$, is dominated by the contribution to the integral (3.14) from the region $s \sim O(\eta^{-1})$. Use of the asymptotic form of G for small arguments yields, in terms of the integration variable $t = \eta s$,

$$M \sim C\eta^{-\sqrt{2}} \int_0^\infty t^{\sqrt{2}-1} J_1(t)\,\mathrm{d}t. \tag{3.18}$$

Evaluation of this integral (Sneddon 1972) gives

$$\varphi^{(0)} \sim C \frac{2^{\sqrt{2}-1}\Gamma\left(\frac{1}{2}(1+\sqrt{2})\right)}{\Gamma\left(\frac{1}{2}(3-\sqrt{2})\right)} \eta^{1-\sqrt{2}} \cos\psi, \tag{3.19}$$

with Γ the Gamma function. Since $\rho \sim 2/\eta$ for $\eta \gg 1$, the electric field is singular in this region. Accordingly, in order to obtain a uniform solution it becomes necessary to separately analyse the gap region, wherein $z \sim O(\delta)$, by rescaling the pertinent variables in this region.

3.2. *Inner solution*

Here, we follow Solomentsev *et al.* (1997). Define the stretched coordinates,

$$Z = z/\delta, \quad R = \rho/\delta^{1/2}, \tag{3.20}$$

which transform the surface of the sphere (3.1) lying in the proximity of the wall into the representation

$$Z = H(R;\delta) \tag{3.21}$$

(see figure 1), wherein

$$H(R;\delta) \sim 1 + \frac{R^2}{2} + \delta\frac{R^4}{8} + \cdots \triangleq H^{(0)}(R) + \delta H^{(1)}(R) + \cdots. \tag{3.22}$$

† Another physical problem possessing the present Neumann-type structure is that posed by the optical polarization of a pair of touching spheres (Paley, Radchik & Smith 1993). While those authors employed tangent-sphere coordinates for the solution of Laplace's equation, their subsequent analysis failed to recognize that the non-homogeneous boundary condition on the sphere is transformed into a differential (rather than algebraic) equation for the Hankel transform of the potential (cf. (3.13)).

In terms of these stretched coordinates, the gradient operator is given by

$$\nabla = \delta^{-1}\boldsymbol{e}_z \frac{\partial}{\partial Z} + \delta^{-1/2}\,\boldsymbol{e}_\rho \frac{\partial}{\partial R} + \delta^{-1/2}\,\boldsymbol{e}_\psi \frac{1}{R}\frac{\partial}{\partial \psi}. \tag{3.23}$$

Thus, the outward (non-unit) normal vector to the sphere is given by

$$\boldsymbol{N} = -\boldsymbol{e}_z + \delta^{1/2}\boldsymbol{e}_\rho \left[\frac{\mathrm{d}H^{(0)}}{\mathrm{d}R} + \delta \frac{\mathrm{d}H^{(1)}}{\mathrm{d}R} + \cdots\right]. \tag{3.24}$$

The boundary-value problem governing $\Phi \equiv \Phi(R, Z, \psi; \delta)$ consists of: (i) the Laplace equation,

$$\frac{\partial^2 \Phi}{\partial Z^2} + \delta\left[\frac{\partial^2 \Phi}{\partial R^2} + \frac{1}{R}\frac{\partial \Phi}{\partial R} + \frac{1}{R^2}\frac{\partial^2 \Phi}{\partial \psi^2}\right] = 0; \tag{3.25}$$

(ii) the boundary condition on the wall,

$$\frac{\partial \Phi}{\partial Z} = 0 \quad \text{at} \quad Z = 0; \tag{3.26}$$

(iii) the boundary condition on the sphere surface,

$$\frac{\partial \Phi}{\partial Z} = \delta\left[\frac{\mathrm{d}H^{(0)}}{\mathrm{d}R} + \delta\frac{\mathrm{d}H^{(1)}}{\mathrm{d}R} + \cdots\right]\frac{\partial \Phi}{\partial R} \quad \text{at} \quad Z = H^{(0)} + \delta H^{(1)} + \cdots; \tag{3.27}$$

and (iv) a regularity condition, requiring the continuity of $\nabla\Phi$ in the limit $R \to 0$.

Obviously, Φ may be expressed as an asymptotic series in powers of δ. However, since Φ satisfies a homogeneous problem (as the far-field condition does not apply within the inner region), any arbitrary pre-factor $\mu(\delta)$ may multiply this series:

$$\Phi(R, Z, \psi; \delta) \sim \mu(\delta)\big[\Phi^{(0)}(R, Z, \psi) + \delta\,\Phi^{(1)}(R, Z, \psi) + \cdots\big]. \tag{3.28}$$

This pre-factor is required for matching with the outer solution. This matching also suggests the following representation:

$$\Phi^{(i)}(R, Z, \psi) = G^{(i)}(R, Z)\cos\psi, \quad i = 0, 1, \ldots. \tag{3.29}$$

The functions $\{G^{(i)}\}_{i=0}^{\infty}$ are governed by: (i) equations

$$\frac{\partial^2 G^{(i)}}{\partial Z^2} = \begin{cases} 0, & i = 0, \\ -\mathscr{L}G^{(i-1)}, & i > 0, \end{cases} \tag{3.30}$$

where $\mathscr{L}$ denotes the operator

$$\mathscr{L} = \frac{\partial^2}{\partial R^2} + \frac{1}{R}\frac{\partial}{\partial R} - \frac{1}{R^2}; \tag{3.31}$$

(ii) the boundary condition on the wall,

$$\frac{\partial G^{(i)}}{\partial Z} = 0 \quad \text{at} \quad Z = 0; \tag{3.32}$$

and (iii) the respective orders of the boundary condition on the sphere,

$$\left[\frac{\partial G^{(0)}}{\partial Z} + \delta\frac{\partial G^{(1)}}{\partial Z} + \cdots\right] = \delta\left[\frac{\mathrm{d}H^{(0)}}{\mathrm{d}R} + \delta\frac{\mathrm{d}H^{(1)}}{\mathrm{d}R} + \cdots\right]\left[\frac{\partial G^{(0)}}{\partial R} + \delta\frac{\partial G^{(1)}}{\partial R} + \cdots\right], \tag{3.33}$$

which is to be evaluated at $Z = H^{(0)}(R) + \delta H^{(1)}(R) + \cdots$.

The $O(1)$ problem is given by

$$\frac{\partial^2 G^{(0)}}{\partial Z^2} = 0 \quad \text{for} \quad 0 \leqslant Z \leqslant H^{(0)}, \tag{3.34a}$$

$$\frac{\partial G^{(0)}}{\partial Z} = 0 \quad \text{at} \quad Z = 0, H^{(0)}, \tag{3.34b}$$

from which it is concluded that $G^{(0)} = G^{(0)}(R)$. The equation governing $G^{(0)}$ is obtained from the solvability condition for the $O(\delta)$ problem,

$$\frac{\partial^2 G^{(1)}}{\partial Z^2} = -\mathscr{L} G^{(0)} \quad \text{for} \quad 0 \leqslant Z \leqslant H^{(0)}, \tag{3.35a}$$

$$\frac{\partial G^{(1)}}{\partial Z} = 0 \quad \text{at} \quad Z = 0, \tag{3.35b}$$

$$\frac{\partial G^{(1)}}{\partial Z} = \frac{\mathrm{d}H^{(0)}}{\mathrm{d}R}\frac{\mathrm{d}G^{(0)}}{\mathrm{d}R} \quad \text{at} \quad Z = H^{(0)}. \tag{3.35c}$$

Specifically, from (3.35a,b) it follows that

$$\frac{\partial G^{(1)}}{\partial Z} = -Z\mathscr{L} G^{(0)}. \tag{3.36}$$

Substitution into (3.35c) yields the second-order homogeneous equation,

$$H^{(0)}\mathscr{L} G^{(0)} + R\frac{\mathrm{d}G^{(0)}}{\mathrm{d}R} = 0. \tag{3.37}$$

One of the solutions of (3.37) was obtained by Solomentsev *et al.* (1997), namely, in present notation,

$$G^{(0)} = DR\left[H^{(0)}(R)\right]^{\beta-1} F\left[1-\beta, 1-\beta, 2, \frac{R^2}{2H^{(0)}(R)}\right], \tag{3.38}$$

where $\beta = 2^{-1/2}$ and D is a constant of integration. This solution is $\sim R$ as $R \to 0$. The other solution, $\sim R^{-1}$ as $R \to 0$, does not satisfy the regularity condition. At the outer edge of the inner domain, where $R \gg 1$,

$$G^{(0)} \sim D\,\frac{2^{1-\beta}\Gamma(\sqrt{2})}{[\Gamma(1+\beta)]^2} R^{\sqrt{2}-1}. \tag{3.39}$$

Matching of this expression with the 'inner' limit of the leading-order outer solution, (3.19), yields $\mu(\delta) = \delta^{(\sqrt{2}-1)/2}$, as well as $D = -1.067437$. These results agree with those of Solomentsev *et al.* (1997), wherein the matching was performed using their exact bipolar-coordinate solution.

The leading-order correction may be obtained along similar lines. From (3.36)–(3.37) it is obvious that

$$G^{(1)}(R, Z) = D^{(1)}(R) - \frac{Z^2}{2}\mathscr{L} G^{(0)}. \tag{3.40}$$

The equation governing $D^{(1)}(R)$ is obtained from the solvability condition for the $O(\delta^2)$ problem, namely

$$\frac{\partial^2 G^{(2)}}{\partial Z^2} = -\mathscr{L} G^{(1)} \quad \text{for} \quad 0 \leqslant Z \leqslant H^{(0)}, \tag{3.41a}$$

$$\frac{\partial G^{(2)}}{\partial Z} = 0 \quad \text{at} \quad Z = 0, \tag{3.41b}$$

$$\frac{\partial G^{(2)}}{\partial Z} = \frac{\mathrm{d}H^{(0)}}{\mathrm{d}R}\frac{\partial G^{(1)}}{\partial R} + \frac{\mathrm{d}H^{(1)}}{\mathrm{d}R}\frac{\mathrm{d}G^{(0)}}{\mathrm{d}R} - H^{(1)}\frac{\partial^2 G^{(1)}}{\partial^2 Z} \quad \text{at} \quad Z = H^{(0)}, \tag{3.41c}$$

which yields the ordinary differential equation

$$\begin{aligned} H^{(0)}\mathscr{L}D^{(1)} + R\frac{\mathrm{d}D^{(1)}}{\mathrm{d}R} &= -H^{(1)}\mathscr{L}G^{(0)} - \frac{\mathrm{d}H^{(1)}}{\mathrm{d}R}\frac{\mathrm{d}G^{(0)}}{\mathrm{d}R} \\ &\quad + \frac{1}{2}\frac{\mathrm{d}H^{(0)}}{\mathrm{d}R}\left[H^{(0)}\right]^2\frac{\mathrm{d}}{\mathrm{d}R}\mathscr{L}G^{(0)} + \frac{1}{6}\left[H^{(0)}\right]^3\mathscr{L}^2G^{(0)}, \end{aligned} \tag{3.42}$$

which possesses the same homogeneous solution as (3.37), namely (3.38). It is easy to verify that

$$D^{(1)}(R) \sim D\frac{2^{1-\beta}\Gamma(\sqrt{2})}{24(1+\sqrt{2})[\Gamma(1+\beta)]^2}R^{\sqrt{2}+1}\{1 + O(R^{-2})\} \quad \text{for} \quad R \gg 1. \tag{3.43}$$

It is only this latter asymptotic behaviour of $D^{(1)}$ that is required in the following analysis.

4. Flow field (c)

The problem governing contribution (c) consists of: (i) the Stokes equations,

$$\nabla \cdot \boldsymbol{v} = 0, \quad \nabla^2 \boldsymbol{v} = \nabla p; \tag{4.1}$$

(ii) the boundary conditions on the sphere and wall,

$$\boldsymbol{v} = (1-\gamma)\nabla\Phi \quad \text{on} \quad \mathscr{P}, \tag{4.2}$$

$$\boldsymbol{v} = \boldsymbol{0} \quad \text{on} \quad \mathscr{W}; \tag{4.3}$$

and (iii) the attenuation condition,

$$\boldsymbol{v} \to \boldsymbol{0} \quad \text{as} \quad |\boldsymbol{x}| \to \infty. \tag{4.4}$$

In principle, one can solve the above boundary-value problem by following the asymptotic scheme of O'Neill & Stewartson (1967), who considered the translation of a sphere in the proximity of a wall. However, the boundary conditions associated with their translation problem were expressed in terms of elementary functions. In contrast, the present boundary conditions involve terms containing derivatives of Φ (cf. (3.7)–(3.8), (3.38)). Given the laborious effort required by O'Neill & Stewartson (1967) towards evaluating their flow fields (and the subsequent integration of the stresses over both the outer and inner regions), a similar approach here would appear to constitute a formidable task.

The *ansatz* for the solution required here utilizes a theorem (Brenner 1964) which enables evaluation of the force and torque without a comparable need for the detailed solution of the pertinent flow equations. The starting point for that computational scheme entails a reciprocal theorem (Happel & Brenner 1965) relating any two sets of flow fields, say $(\boldsymbol{v}', \boldsymbol{\pi}')$ and $(\boldsymbol{v}'', \boldsymbol{\pi}'')$, each individually satisfying the incompressible creeping flow and continuity equations within the same arbitrary fluid domain $\mathscr{V}$

bounded by the closed surface $\partial\mathscr{V}$. Explicitly,

$$\int_{\partial\mathscr{V}} \mathrm{d}S\, \boldsymbol{n}\cdot\boldsymbol{\pi}'\cdot\boldsymbol{v}'' = \int_{\partial\mathscr{V}} \mathrm{d}S\, \boldsymbol{n}\cdot\boldsymbol{\pi}''\cdot\boldsymbol{v}'. \tag{4.5}$$

In the case of a body immersed in a flow in rest at infinity, with a wall present in the proximity of the body, $\partial\mathscr{V}$ may be taken as the union of the the boundary of the body, $\mathscr{P}$, and the surface of the wall, $\mathscr{W}$.† Consider such a configuration, with velocity field $\widetilde{\boldsymbol{v}}$ prescribed on $\mathscr{P}$, and with zero velocity on $\mathscr{W}$. Based upon the reciprocal theorem, the force and torque on the particle, say $\widetilde{\boldsymbol{F}}$ and $\widetilde{\boldsymbol{T}}$, may each be expressed as simple quadratures of $\widetilde{\boldsymbol{v}}$ over the particle surface. Those results, expressed in the present dimensionless notation, are embodied in the following quadratures:

$$\widetilde{F}_k = \frac{1}{6\pi}\oint_{\mathscr{P}} \mathrm{d}S\, n_i\, \overline{\Pi}_{ijk}\, \widetilde{v}_j, \qquad \widetilde{T}_k = \frac{1}{8\pi}\oint_{\mathscr{P}} \mathrm{d}S\, n_i\, \overline{\overline{\Pi}}_{ijk}\, \widetilde{v}_j, \tag{4.6}$$

wherein $\overline{\boldsymbol{\Pi}} = \boldsymbol{e}_i\, \boldsymbol{e}_j\, \boldsymbol{e}_k\, \overline{\Pi}_{ijk}$ and $\overline{\overline{\boldsymbol{\Pi}}} = \boldsymbol{e}_i\, \boldsymbol{e}_j\, \boldsymbol{e}_k\, \overline{\overline{\Pi}}_{ijk}$ denote the respective translational and rotational triadic 'stress' fields (Happel & Brenner 1965) which depend, apart from the position vector $\boldsymbol{x}$, only upon the geometry of the particle–wall configuration. Explicitly, the dyadic stress field arising from translational motion of the particle with an arbitrary velocity $\boldsymbol{U}$ is given by $\overline{\boldsymbol{\Pi}}\cdot\boldsymbol{U}$; similarly, the dyadic stress field arising from rotational motion of the particle with an arbitrary angular velocity $\boldsymbol{\Omega}$ is given by $\overline{\overline{\boldsymbol{\Pi}}}\cdot\boldsymbol{\Omega}$. The scalar x- and y-components of $\widetilde{\boldsymbol{F}}$ and $\widetilde{\boldsymbol{T}}$ are, therefore,

$$\widetilde{F}_1 = \frac{1}{6\pi}\oint_{\mathscr{P}} \mathrm{d}S\, \boldsymbol{n}\cdot\boldsymbol{\pi}_{\mathrm{tr}}\cdot\widetilde{\boldsymbol{v}}, \qquad \widetilde{T}_2 = \frac{1}{8\pi}\oint_{\mathscr{P}} \mathrm{d}S\, \boldsymbol{n}\cdot\boldsymbol{\pi}_{\mathrm{rot}}\cdot\widetilde{\boldsymbol{v}}. \tag{4.7}$$

In the above, $\boldsymbol{\pi}_{\mathrm{tr}}$ is the dyadic stress field arising from translational motion of the sphere with a unit velocity in the x-direction in a fluid at rest on $\mathscr{W}$ and at infinity. Similarly, $\boldsymbol{\pi}_{\mathrm{rot}}$ is the stress field arising from rotational motion of the sphere, about its centre, with a unit angular velocity in the y-direction, in a fluid at rest on $\mathscr{W}$ and at infinity. Explicitly, if the flow fields $(\boldsymbol{v}_{\mathrm{tr}}, p_{\mathrm{tr}})$ and $(\boldsymbol{v}_{\mathrm{rot}}, p_{\mathrm{rot}})$ respectively satisfy the following boundary conditions:

$$\begin{aligned}
&\boldsymbol{v}_{\mathrm{tr}} = \boldsymbol{e}_x \quad \text{on} \quad \mathscr{P}, && \boldsymbol{v}_{\mathrm{rot}} = \boldsymbol{e}_y \times (\boldsymbol{x} - \boldsymbol{x}_O) \quad \text{on} \quad \mathscr{P},\\
&\boldsymbol{v}_{\mathrm{tr}} = \boldsymbol{0} \quad \text{on} \quad \mathscr{W}, && \boldsymbol{v}_{\mathrm{rot}} = \boldsymbol{0} \quad \text{on} \quad \mathscr{W},\\
&\boldsymbol{v}_{\mathrm{tr}} \to \boldsymbol{0} \quad \text{as} \quad |\boldsymbol{x}| \to \infty, && \boldsymbol{v}_{\mathrm{rot}} \to \boldsymbol{0} \quad \text{as} \quad |\boldsymbol{x}| \to \infty,
\end{aligned}$$

then the stress fields $\boldsymbol{\pi}_{\mathrm{tr}}$ and $\boldsymbol{\pi}_{\mathrm{rot}}$ are simply given by the constitutive expression (2.11), with $(\boldsymbol{v}, p)$ respectively replaced by $(\boldsymbol{v}_{\mathrm{tr}}, p_{\mathrm{tr}})$ and $(\boldsymbol{v}_{\mathrm{rot}}, p_{\mathrm{rot}})$. This result (in a more general form) was used by Goldman, Cox & Brenner (1967*b*) to evaluate the force and torque on a stationary sphere near a plane wall in the presence of a uniform shear flow far from the sphere.

As the velocity field (c) vanishes on the wall and at infinity, the theorem may be used with $(1-\gamma)\nabla\Phi$ substituted for $\widetilde{\boldsymbol{v}}$ in (4.7), yielding

$$F = (1-\gamma) f_{\mathrm{el}}(\delta), \qquad T = (1-\gamma) g_{\mathrm{el}}(\delta), \tag{4.8}$$

† The contribution from the boundary at infinity vanishes under very moderate conditions imposed upon both $\boldsymbol{v}'$ and $\boldsymbol{v}''$ – say, attenuation at least as fast as $|\boldsymbol{x}|^{-1}$. These conditions are virtually always satisfied.

wherein the force and torque coefficients are given by the surface quadratures

$$f_{el}(\delta) = \frac{1}{6\pi} \oint_{\mathscr{P}} dS\, \boldsymbol{n} \cdot \boldsymbol{\pi}_{tr} \cdot \nabla \Phi, \tag{4.9}$$

$$g_{el}(\delta) = \frac{1}{8\pi} \oint_{\mathscr{P}} dS\, \boldsymbol{n} \cdot \boldsymbol{\pi}_{rot} \cdot \nabla \Phi. \tag{4.10}$$

Note that these expressions are valid for any gap width (not necessarily small).†

The hydrodynamic fields, $\boldsymbol{\pi}_{tr}$ and $\boldsymbol{\pi}_{rot}$, as well as the electric potential have been evaluated for both arbitrary and small separations, enabling the evaluation of F and T in both cases. Effecting the respective quadratures (4.9) and (4.10) using the exact bipolar-coordinates expressions for φ, $\boldsymbol{\pi}_{tr}$ and $\boldsymbol{\pi}_{rot}$ is straightforward. The exact solution for φ was obtained by Keh & Chen (1989), whereas the respective solutions for the translational and rotational flow fields were derived by O'Neill (1964) and Dean & O'Neill (1963). We have reconstructed these solutions for δ as small as 0.005 and evaluated $f_{el}(\delta)$ and $g_{el}(\delta)$ via appropriate integrations in bipolar coordinates.

Consider now the case of small separation, for which the electric field has been evaluated in the previous two sections. The 'translational' flow field, $(\boldsymbol{v}_{tr}, p_{tr})$, for the small-gap geometric configuration, has already been evaluated by O'Neill & Stewartson (1967), and the comparable 'rotational' field, $(\boldsymbol{v}_{rot}, p_{rot})$, by Cooley & O'Neill (1968). These fields were evaluated in both the inner and outer regions. Thus, in principle, the force (and torque) may be represented as the sum of respective inner and outer contributions, expressed as integrals over complementary domains on the sphere surface. The integration in the inner contribution is carried out over the range $\rho \leqslant \rho_0$, with $\delta^{1/2} \ll \rho_0 \ll 1$ denoting a value lying within the 'intermediate region' where the matching takes place. The respective integration in the outer contribution is performed over the interval $0 \leqslant \eta \leqslant \eta_0$, with η_0 denoting the value of the outer variable η corresponding to ρ_0. (To leading order, $\eta_0 = 2\rho_0/(1+\rho_0^2)$.)

Consider first the force acting on the sphere, given by (4.9). We begin with the calculation of the inner contribution. Within the gap, the translational velocity and pressure fields are represented by the respective forms (O'Neill & Stewartson 1967)

$$\boldsymbol{v}_{tr}(R,\psi,Z) = \boldsymbol{e}_\rho U(R,Z)\cos\psi + \boldsymbol{e}_\psi V(R,Z)\sin\psi + \boldsymbol{e}_z W(R,Z)\cos\psi, \tag{4.11}$$

$$p_{tr}(R,\psi,Z) = P(R,Z)\cos\psi. \tag{4.12}$$

The corresponding stress field, $\boldsymbol{\pi}_{tr}$, is evaluated using (2.11); the traction at a point on the sphere surface is given, in terms of the functions (U, V, W) and P, by the expression

$$\begin{aligned}\boldsymbol{n}\cdot\boldsymbol{\pi}_{tr} = {} & \boldsymbol{e}_\rho\left[\left(-P + 2\delta^{-1/2}\frac{\partial U}{\partial R}\right)\sin\chi - \left(\delta^{-1}\frac{\partial U}{\partial Z} + \delta^{-1/2}\frac{\partial W}{\partial R}\right)\cos\chi\right]\cos\psi \\ & + \boldsymbol{e}_\psi\left[\left(\delta^{-1/2}R\frac{\partial}{\partial R}\left(\frac{V}{R}\right) - \delta^{-1/2}\frac{U}{R}\right)\sin\chi - \left(\delta^{-1}\frac{\partial V}{\partial Z} - \delta^{-1/2}\frac{W}{R}\right)\cos\chi\right]\sin\psi \\ & + \boldsymbol{e}_z\left[\left(\delta^{-1}\frac{\partial U}{\partial Z} + \delta^{-1/2}\frac{\partial W}{\partial R}\right)\sin\chi + \left(P - 2\delta^{-1}\frac{\partial W}{\partial Z}\right)\cos\chi\right]\cos\psi,\end{aligned} \tag{4.13}$$

† An alternative use of the reciprocal theorem appears in the work of Teubner (1982), expressing the force and torque acting on a body as linear functionals of the electric field. That work, which is not limited to thin Debye layers, entails the exact flow and electric equations, taking into account electrical body forces. The resulting force and torque expressions therefore involve volume – rather than surface – integrals. However, since in the general case the electric field is coupled to the fluid motion, these results are only formal and do not remove the need to solve the flow field.

with $\pi-\chi$ the polar angle between the radius vector to the sphere surface from its centre and the z-axis, wherein $\sin\chi=\delta^{1/2}R$, and the outward normal unit vector $\boldsymbol{n}$ on the sphere given by $\boldsymbol{e}_\rho \sin\chi-\boldsymbol{e}_z\cos\chi$. The fields (U, V, W) and P have the respective asymptotic forms

$$U(R, Z;\delta)=U^{(0)}(R, Z)+\delta U^{(1)}(R, Z)+\cdots, \tag{4.14a}$$

$$V(R, Z;\delta)=V^{(0)}(R, Z)+\delta V^{(1)}(R, Z)+\cdots, \tag{4.14b}$$

$$W(R, Z;\delta)=\delta^{1/2}\left[W^{(0)}(R, Z)+\delta W^{(1)}(R, Z)+\cdots\right], \tag{4.14c}$$

$$P(R, Z;\delta)=\delta^{-3/2}\left[P^{(0)}(R, Z)+P^{(1)}(R, Z)+\cdots\right], \tag{4.14d}$$

in which the functions $[U^{(0)}, V^{(0)}, W^{(0)}]$ and $P^{(0)}$ were explicitly evaluated by O'Neill & Stewartson (1967).

In terms of the stretched gap variables, the inner integration is carried out over the range $R\leqslant R_0$, with $1\ll R_0\ll\delta^{-1/2}$. Substitution of the expansions (4.14) and (3.28) into (4.13) and (4.9), in conjunction with the sphere surface equation, (3.22), and the expression

$$\mathrm{d}S=\sin\chi\,\mathrm{d}\chi\,\mathrm{d}\psi\sim\delta\left[1+\delta\frac{R^2}{2}+O(\delta^2)\right]R\,\mathrm{d}R\,\mathrm{d}\psi \tag{4.15}$$

for the area element, enables the inner contribution to f_{el} to be expressed by the asymptotic expansion

$$f_{el}^{\text{inner}}(\delta;R_0)\sim\delta^{-1/2}\mu(\delta)\int_0^{R_0}\left[\mathscr{F}^{(0)}(R)+\delta\mathscr{F}^{(1)}(R)+O(\delta^2)\right]\mathrm{d}R. \tag{4.16}$$

The leading-order term in this integrand is given by

$$\mathscr{F}^{(0)}(R)=\frac{R}{6}\left[P^{(0)}\frac{\partial G^{(1)}}{\partial Z}-RP^{(0)}\frac{\mathrm{d}G^{(0)}}{\mathrm{d}R}-\frac{\partial U^{(0)}}{\partial Z}\frac{\mathrm{d}G^{(0)}}{\mathrm{d}R}+\frac{\partial V^{(0)}}{\partial Z}\frac{G^{(0)}}{R}\right]_{Z=H^{(0)}(R)}. \tag{4.17}$$

Upon making use of (3.35c) together with the explicit expressions for the functions $[U^{(0)}, V^{(0)}, W^{(0)}]$ and $P^{(0)}$ (O'Neill & Stewartson 1967), one obtains

$$\mathscr{F}^{(0)}(R)=\frac{4}{15}\left[\frac{R^2-4}{2R^2+4}\frac{\mathrm{d}G^{(0)}}{\mathrm{d}R}-\frac{G^{(0)}}{R}\right]\frac{R}{H^{(0)}(R)}. \tag{4.18}$$

Since this term varies like $R^{\sqrt{2}-3}$ for large R, it is allowable to set $R_0=\infty$ in (4.16) in order to evaluate the integral of $\mathscr{F}^{(0)}$, say a_0. The integral was evaluated using the expressions (3.38) and (3.39), yielding $a_0=0.99337$. Thus, the leading-order inner contribution to the force is

$$f_{el}^{\text{inner}^{(0)}}(\delta)=a_0\delta^{\sqrt{2}/2-1}. \tag{4.19}$$

Observe, as $\delta\to 0$, that this term dominates those resulting from translation and rotation, which diverge only as $\log\delta$ (cf. (6.5)–(6.6)). The fact that this result does not depend upon R_0 signals that no comparable contribution to the force arises from the outer region. Indeed, consider the leading-order outer contribution to the force, which may in principle be expressed as an integral over η in the range $0\leqslant\eta<\eta_0$. As δ does not appear in the leading-order outer problem, this integral can depend only upon η_0, say $I(\eta_0)$. If $\lim_{\eta_0\to\infty}I(\eta_0)$ exists, the integral is $O(1)$, and thus subdominant to (4.19). Otherwise, the arbitrariness in the choice of η_0 requires that the (presumably divergent) η_0-dependent terms, expressed in terms of the inner variable R_0 by the relation $\eta_0=\eta_0(\delta, R_0)$, be cancelled by comparable terms arising from the inner contribution to the force; but this is impossible as the inner leading-order contribution to the force (4.19) does not depend upon R_0. We thus conclude that the outer contribution to the force is at most of $O(1)$.

It still remains to estimate the next-order contribution from the inner region. In order to evaluate $\mathscr{F}^{(1)}$, explicit expressions for the functions $[U^{(1)}, V^{(1)}, W^{(1)}]$ and $P^{(1)}$ are required. However, these fields were evaluated by O'Neill & Stewartson only for $R \gg 1$. Using their expressions in conjunction with (3.39) and (3.43) it may be verified that

$$\mathscr{F}^{(1)}(R) \sim AR^{\sqrt{2}-1}[1 + O(R^{-2})] \quad \text{for} \quad R \gg 1, \tag{4.20}$$

where the constant A depends upon the asymptotic leading-order behaviour of the translational inner flow field for $R \gg 1$. Thus, the leading-order inner correction to the force is given in the form

$$f_{\mathrm{el}}^{\mathrm{inner}(1)}(\delta) = \delta^{\sqrt{2}/2}\left[A_1 R_0^{\sqrt{2}} + A_2\right], \tag{4.21}$$

wherein $A_1 = A/\sqrt{2}$ and the constant A_2 depends upon the overall properties of the inner fields. (As the total force cannot depend upon the arbitrary parameter R_0, it is obvious that the first term of (4.21) must be cancelled out by a corresponding term from the outer contribution, namely $-(1-\gamma)A_1\rho_0^{\sqrt{2}}$.) Note that $F^{(1)}$ is $o(1)$ for $\delta \ll 1$. Consequently, the total force resulting from the electrically induced flow field (c) is given by the expression

$$f_{\mathrm{el}}(\delta) \sim \left[a_0\delta^{\sqrt{2}/2-1} + a_1 + o(1)\right], \tag{4.22}$$

with a_1 dependent upon the overall properties of the outer fields.

Similar arguments apply to evaluation of the torque, given by (4.10). The rotational flow field (Cooley & O'Neill 1968) possesses the same structure as the translational field, namely (4.11)–(4.14). Thus, the inner contribution to the torque is expressed in a form similar to (4.16) as

$$g_{\mathrm{el}}^{\mathrm{inner}}(\delta) = \delta^{-1/2}\mu(\delta)\int_0^{R_0}\left[\mathscr{T}^{(0)}(R) + \delta\mathscr{T}^{(1)}(R) + \cdots\right]\mathrm{d}R, \tag{4.23}$$

with $\mathscr{T}^{(0)}(R)$ given by the same expression as is $\mathscr{F}^{(0)}$, namely (4.17). Use of the 'rotational' expressions for the functions $[U^{(0)}, V^{(0)}, W^{(0)}]$ and $P^{(0)}$ (Cooley & O'Neill 1968) yields

$$\mathscr{T}^{(0)}(R) = \frac{1}{20}\left[\frac{G^{(0)}}{R} + \frac{2+7R^2}{2+R^2}\frac{\mathrm{d}G^{(0)}}{\mathrm{d}R}\right]\frac{R}{H^{(0)}(R)}. \tag{4.24}$$

As with (4.18), this expression may be integrated by setting $R_0 = \infty$, yielding $-3a_0/4$. The torque coefficient, associated with the 'electrical' flow (c), is therefore given by

$$g_{\mathrm{el}}(\delta) \sim \left[b_0\delta^{\sqrt{2}/2-1} + b_1 + o(1)\right], \tag{4.25}$$

with $b_0 = -3a_0/4$ and with b_1 depending upon the overall properties of the outer fields.

In principle, the coefficients a_1 and b_1 can be obtained via evaluation of the integrals (4.9) and (4.10) over the outer region. This, however, turns out to be extremely difficult since both the outer (translational and rotational) flow fields, and the outer electric potential, are expressed as Hankel transforms (cf. (3.7)–(3.8)). Instead, we employ the more straightforward approach of Goldman *et al.* (1967*a*), evaluating these coefficients via 'patching' of the asymptotic expressions (4.22) and (4.25) with their corresponding 'exact' values. The latter have been obtained by effecting the respective quadratures (4.9) and (4.10) using the exact bipolar-coordinates expressions for φ, $\boldsymbol{\pi}_{tr}$ and $\boldsymbol{\pi}_{rot}$. From these exact values we derived the approximate results, $a_1 \approx 0.3224$ and $b_1 \approx 1.1742$.

5. Flow field (d)

In terms of the resulting forces and torques, flow field (d) is equivalent to that obtained via a Galilean transformation involving the velocity $\gamma \nabla \Phi_\infty = -\gamma \boldsymbol{e}_x$. The problem governing the transformed field consists of: (i) the flow equations,

$$\nabla \cdot \boldsymbol{v} = 0, \quad \nabla^2 \boldsymbol{v} = \nabla p; \tag{5.1}$$

(ii) the boundary conditions on the sphere and wall,

$$\boldsymbol{v} = \gamma \nabla \varphi \quad \text{on} \quad \mathscr{P}, \tag{5.2}$$

$$\boldsymbol{v} = \gamma \nabla \varphi \quad \text{on} \quad \mathscr{W}; \tag{5.3}$$

and (iii) the attenuation condition,

$$\boldsymbol{v} \to \boldsymbol{0} \quad \text{as} \quad |\boldsymbol{x}| \to \infty. \tag{5.4}$$

As any (solenoidal) irrotational flow field automatically satisfies Stokes equations, it is obvious that the solution of problem (d) is simply

$$\boldsymbol{v} \equiv \gamma \nabla \varphi, \qquad p \equiv 0. \tag{5.5}$$

The corresponding stress field is

$$\boldsymbol{\pi} = 2\gamma \nabla \nabla \varphi. \tag{5.6}$$

Consider the hydrodynamic force on the sphere resulting from this field. Since this field is divergence-free, the integral appearing in (2.12) may be evaluated over any arbitrary surface within the fluid domain that encloses the sphere. It is convenient to choose the domain of integration as constituting the union of two surfaces – the first being the disk ($0 \leqslant \rho \leqslant \rho_0$, $z = 0$, $0 \leqslant \psi \leqslant 2\pi$) located on the wall, and the second chosen as the hemisphere, $\rho^2 + z^2 = r_\infty^2$ (with $z > 0$). Since $\varphi \sim O(|\boldsymbol{x}|^{-2})$ for large $|\boldsymbol{x}|$, the hemisphere contribution vanishes as $r_\infty \to \infty$. The force $\boldsymbol{F}$ is therefore opposite in sign to the hydrodynamic force acting on the wall, the latter being given by the expression

$$\boldsymbol{F}_w = 2\gamma \int_{\mathscr{W}} \mathrm{d}S \, \boldsymbol{e}_z \cdot \nabla \nabla \varphi. \tag{5.7}$$

In terms of circular cylindrical coordinates,

$$\boldsymbol{F}_w = -2\gamma \int_0^{2\pi} \mathrm{d}\psi \int_0^\infty \mathrm{d}\rho \, \rho \left[\frac{\partial}{\partial z} (\nabla \varphi) \right]_{z=0}. \tag{5.8}$$

This expression vanishes owing to the $\cos \psi$ azimuthal dependence of φ. Thus, the force on the wall (and, consequently, on the sphere) vanishes identically. Since the azimuthal dependence of the electric potential upon ψ reflects the geometric symmetry of the particle–wall configuration, it is obvious that this result is true for any gap width (not necessarily small).

Next, consider the dimensionless torque on the sphere, which is most conveniently expressed in terms of the position vector $\boldsymbol{r} = \boldsymbol{x} - \boldsymbol{x}_O$ relative to the sphere centre (cf. (2.13)),

$$\boldsymbol{T} = 2\gamma \oint_{\mathscr{P}} \mathrm{d}S\, \boldsymbol{r} \times (\boldsymbol{n} \cdot \nabla\nabla\varphi). \tag{5.9}$$

To evaluate this torque we employ a spherical polar coordinate system, (r, χ, ψ), centred about $\boldsymbol{x}_O$. The gradient operator, expressed in this system, may be written in the form

$$\nabla = \boldsymbol{e}\frac{\partial}{\partial r} + \frac{1}{r}\nabla_{\boldsymbol{e}}, \tag{5.10}$$

where $\boldsymbol{e} = \boldsymbol{r}/r$ is a radial unit vector and the operator,

$$\nabla_{\boldsymbol{e}} = \boldsymbol{e}_\chi \frac{\partial}{\partial \chi} + \boldsymbol{e}_\psi \frac{1}{\sin\chi}\frac{\partial}{\partial \psi}, \tag{5.11}$$

represents differentiation along the unit sphere surface, $\mathscr{P}$. On this surface, where $r = 1$, it follows that $\boldsymbol{r} = \boldsymbol{n} = \boldsymbol{e}$. Hence,

$$\begin{aligned} \boldsymbol{T} &= 2\gamma \int_{\mathscr{P}} \mathrm{d}S\, \boldsymbol{e} \times \frac{\partial}{\partial r}(\nabla\varphi) \\ &= 2\gamma \int_{\mathscr{P}} \mathrm{d}S\, \boldsymbol{e} \times \left[\boldsymbol{e}\frac{\partial^2\varphi}{\partial r^2} + \frac{1}{r}\nabla_{\boldsymbol{e}}\left(\frac{\partial\varphi}{\partial r}\right) - \frac{1}{r^2}\nabla_{\boldsymbol{e}}\varphi\right] \\ &= 2\gamma \int_{\mathscr{P}} \mathrm{d}S\, \boldsymbol{e} \times \left[\nabla_{\boldsymbol{e}}\left(\frac{\partial\varphi}{\partial r}\right) - \nabla_{\boldsymbol{e}}\varphi\right]. \end{aligned} \tag{5.12}$$

However, owing to the boundary condition (2.4), $(\partial\varphi/\partial r)_{r=1} = \boldsymbol{e} \cdot \boldsymbol{e}_x$. Since the operator $\nabla_{\boldsymbol{e}}$ is r-independent, it is permissible to exchange the respective orders of the differentiation and evaluation at $r = 1$, yielding

$$\left[\nabla_{\boldsymbol{e}}\left(\frac{\partial\varphi}{\partial r}\right)\right]_{r=1} = \nabla_{\boldsymbol{e}}\left[\left(\frac{\partial\varphi}{\partial r}\right)_{r=1}\right] = (\nabla_{\boldsymbol{e}}\, \boldsymbol{e}) \cdot \boldsymbol{e}_x = (\boldsymbol{I} - \boldsymbol{ee}) \cdot \boldsymbol{e}_x. \tag{5.13}$$

Thus, $\boldsymbol{T}$ may be expressed as the difference of two integrals,

$$\boldsymbol{T} = 2\gamma \oint_{\mathscr{P}} \mathrm{d}S\, \boldsymbol{e} \times \boldsymbol{e}_x - 2\gamma \oint_{\mathscr{P}} \mathrm{d}S\, \boldsymbol{e} \times \nabla_{\boldsymbol{e}}\varphi. \tag{5.14}$$

The first integral vanishes owing to the antisymmetry of the integrand with respect to $\mathscr{P}$. To evaluate the second integral, note that φ must possess the functional form $\phi(\chi)\cos\psi$ on $r = 1$ (cf. (3.7), (3.29)). Consequently,

$$\begin{aligned} \oint_{\mathscr{P}} \mathrm{d}S\, \boldsymbol{e} \times \nabla_{\boldsymbol{e}}\varphi &= -\int_0^{2\pi} \mathrm{d}\psi \int_0^{\pi} \mathrm{d}\chi\, \sin\chi \left[\boldsymbol{e}_\psi \phi'(\chi)\cos\psi + \boldsymbol{e}_\chi \frac{\phi(\chi)}{\sin\chi}\sin\psi\right] \\ &= -\pi \boldsymbol{e}_y \int_0^{\pi} [\phi'(\chi)\sin\chi + \phi(\chi)\cos\chi]\, \mathrm{d}\chi. \end{aligned} \tag{5.15}$$

Integration by parts reveals that this integral also vanishes. Thus, no torque is exerted on the sphere. As with the force, this result holds true for any gap width.

Since $\nabla\nabla\varphi$ is a divergence-free symmetric dyadic, and since the integrand of (5.9) appears to attenuate as $O(|\boldsymbol{x}|^{-3})$ for large $|\boldsymbol{x}|$ (cf. (3.17)), it seems plausible that Gauss's theorem may be applied, so as to transform the integral (5.9) into one performed over the wall. One would then expect the resulting torque (about the sphere centre) on the wall to also vanish. However, this does not turn out to be the case. The evaluation of the torque acting on the wall, as well as the rationalization of this apparent paradox, are outlined in the Appendix.

We conclude that flow field (d) exerts neither a force nor a torque on the sphere. Considering the form of the boundary conditions applicable to problems (a)–(c), it may be concluded that both the translational and rotational electrophoretic mobilities are proportional to $1-\gamma$ (or, in dimensional notation, to $\zeta_p - \zeta_w$). This result holds for any gap width (cf. (6.3)). This proportionality was suggested by Keh & Chen (1989), based upon their numerical results.

We have not yet been able to establish whether the source of the null contributions of part (d) to the force and torque on the sphere is a consequence of the geometrical symmetry of the sphere–wall geometry (which has been exploited in the foregoing derivation), or is actually a more general result for all irrotational flow fields, which holds irrespective of the specific particle–boundary configuration. In a separate paper (Yariv & Brenner 2003) we have demonstrated that this same null result also holds for the case of a sphere eccentrically positioned within a circular cylinder. Again, however, that geometry possesses several symmetry properties (which were used throughout that analysis).

It is, of course, well known that irrotational Stokes flow does not exert a force on a body in an unbounded fluid (Morrison 1970). As such, it is tempting to believe that this result can easily be extended to the case where boundaries are present. However, Morrison's (1970) proof invokes the rapid attenuation of irrotational flow fields at infinity (Batchelor 1967) (in a manner similar to that involved in the proof of d'Alembert's paradox in inviscid fluid-flow theory, where the forces arise from pressure variations rather than from viscous friction). Obviously, this attenuation argument does not guarantee the absence of forces or torques in the presence of boundaries, as the pertinent surface integrals cannot be extended to infinity. (Indeed, for the comparable problem of a bubble moving through an inviscid liquid, the velocity field is also irrotational; nevertheless, the presence of boundaries results in a net force on the bubble (Miloh 1977).)

6. Results and discussion

Although the ultimate focus of the present paper is the asymptotic limiting case $\delta \ll 1$, it proves worthwhile to first discuss the structure of the mobility expressions for the case of arbitrary (not necessarily small) sphere–wall separations. Such an approach, which elucidates the various elements entering into the electrophoretic motion, is supported by the generality of the problem formulation in §2 (and, specifically, the decomposition of the overall motion into the respective components (a)–(d)).

Since contributions (c) to the force and torque are respectively directed in the x- and y-directions, it is obvious that a force- and couple-free particle will respectively translate parallel to and rotate about axes in these directions. Thus, in evaluating the forces and torques in problems (a) and (b), one need only consider the respective cases $\boldsymbol{U} = U\boldsymbol{e}_x$ and $\boldsymbol{\Omega} = \Omega\boldsymbol{e}_y$ (see also the discussion following (2.13)). The force and torque (about the sphere centre) acting on a non-rotating sphere translating with velocity U parallel to a nearby wall are represented by the respective forms $f_{\mathrm{tr}}(\delta)U$ and $g_{\mathrm{tr}}(\delta)U$. Similarly, the force and torque on a non-translating sphere rotating with velocity Ω about an axis parallel to the wall are represented as $f_{\mathrm{rot}}(\delta)\,\Omega$ and $g_{\mathrm{rot}}(\delta)\,\Omega$. The functions $f_{\mathrm{tr}}(\delta)$, $g_{\mathrm{tr}}(\delta)$, $f_{\mathrm{rot}}(\delta)$ and $g_{\mathrm{rot}}(\delta)$, which correspond to translation and rotation with unit velocities, are independent of the respective magnitudes of the sphere velocities. Rather, they only depend upon the sphere–wall geometric configuration, lumped into the single geometric parameter δ. The 'exact' series expressions for $f_{\mathrm{tr}}(\delta)$

and $g_{tr}(\delta)$, valid for arbitrary values of δ, are provided by O'Neill (1964); comparable expressions for $f_{rot}(\delta)$ and $g_{rot}(\delta)$ are given by Dean & O'Neill (1963).

It is obvious from the structure of the 'electrical' problem (c), defined by (4.1)–(4.4), that the corresponding force and torque are proportional to $1-\gamma$, namely

$$(1-\gamma)\, f_{el}(\delta), \quad (1-\gamma)\, g_{el}(\delta).$$

The exact expressions for $f_{el}(\delta)$ and $g_{el}(\delta)$, appropriate for arbitrary values of δ, were evaluated (in the form of numerical quadratures) using the respective bipolar-coordinate expressions for the translational (O'Neill 1964) and rotational (Dean & O'Neill 1963) flow fields (see § 4). Their asymptotic counterparts (cf. (4.22) and (4.25)) were evaluated using the respective small-gap flow fields.

Since flow field (d) does not contribute any force or torque, the total force and torque acting on the translating–rotating sphere in the present problem are given by the expressions

$$F = U\, f_{tr}(\delta) + \Omega\, f_{rot}(\delta) + (1-\gamma)\, f_{el}(\delta), \tag{6.1}$$

$$T = U\, g_{tr}(\delta) + \Omega\, g_{rot}(\delta) + (1-\gamma)\, g_{el}(\delta). \tag{6.2}$$

The respective translational and angular velocities of a force- and couple-free sphere are therefore

$$\frac{U}{1-\gamma} = \frac{f_{rot}(\delta)\, g_{el}(\delta) - g_{rot}(\delta)\, f_{el}(\delta)}{f_{tr}(\delta)\, g_{rot}(\delta) - f_{rot}(\delta)\, g_{tr}(\delta)}, \tag{6.3}$$

$$\frac{\Omega}{1-\gamma} = \frac{g_{tr}(\delta)\, f_{el}(\delta) - f_{tr}(\delta)\, g_{el}(\delta)}{f_{tr}(\delta)\, g_{rot}(\delta) - f_{rot}(\delta)\, g_{tr}(\delta)}. \tag{6.4}$$

Consider now the asymptotic limit, $\delta \ll 1$. The force and torque on a non-rotating sphere translating with unit velocity parallel to a nearby wall were obtained by O'Neill & Stewartson (1967). In present notation, they are given by the respective expressions

$$f_{tr}(\delta) = \tfrac{8}{15}\log\delta - 0.95429 + o(1), \quad g_{tr}(\delta) = -\tfrac{1}{10}\log\delta - 0.19296 + o(1). \tag{6.5}$$

The comparable results for a non-translating sphere rotating with a unit angular velocity about an axis parallel to the wall are (Cooley & O'Neill 1968)

$$f_{rot}(\delta) = -\tfrac{2}{15}\log\delta - 0.25725 + o(1), \quad g_{rot}(\delta) = \tfrac{2}{5}\log\delta - 0.37085 + o(1). \tag{6.6}$$

The approximations for $f_{el}(\delta)$ and $f_{el}(\delta)$, calculated in § 4, are

$$f_{el}(\delta) = a_0\delta^{\sqrt{2}/2-1} + 0.3224 + o(1), \quad g_{el}(\delta) = -\frac{3a_0}{4}\delta^{\sqrt{2}/2-1} + 1.1742 + o(1), \tag{6.7}$$

with $a_0 = 0.99337$.

The small-gap approximations for the mobilities are obtained by substitution of (6.5)–(6.7) into (6.3). In the limit $\delta \to 0$ these become, to terms of dominant order,

$$\frac{U}{1-\gamma} = \frac{\Omega}{1-\gamma} \sim -\frac{3a_0}{2}\frac{\delta^{\sqrt{2}/2-1}}{\log\delta}, \tag{6.8}$$

indicating a large translational velocity in the x-direction and an equally large angular velocity in the negative y-direction. These trends agree with the numerical results of Keh & Chen (1989) as their gap width becomes small. Thus, the presence of the wall results in a major enhancement of the sphere's electrophoretically driven velocity.

The exact translational mobility as function of δ is evaluated via substitution into (6.3) of the exact expressions for the coefficients $f_{tr}(\delta), \ldots, g_{el}(\delta)$. The resulting

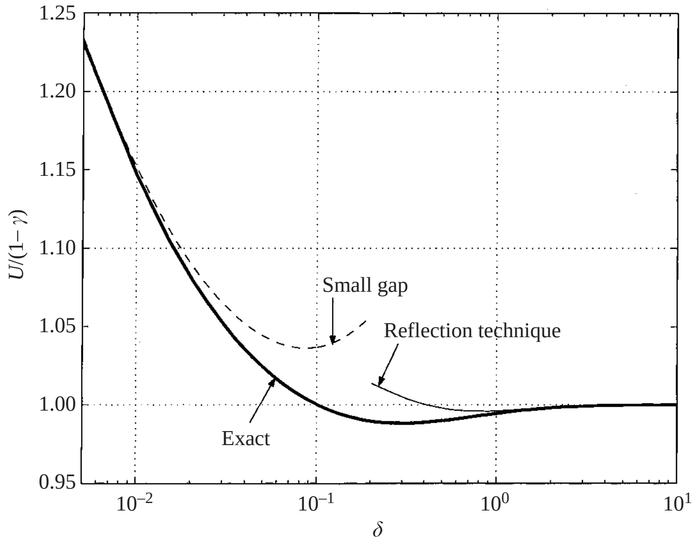

FIGURE 3. Electrophoretic mobility, $U/(1-\gamma)$, as function of δ: —, 'exact'; - - -, small-gap approximation; —, large-gap approximation (Keh & Anderson 1985).

numerical values agree with those provided by Keh & Chen (1989). (Note, however, that these authors have evaluated the exact detailed electrokinetic flow field. The present solution scheme, which makes use of the reciprocal theorem, involves only quadrature of known fields and does not require the comparable solution of partial differential equations. As such, it is expected to provide more accurate results.) Figure 3 displays the variation with δ of this mobility, as well as the corresponding small-gap approximation. Also depicted is the asymptotic approximation for large sphere–wall separations ($\delta \gg 1$),

$$1 - \tfrac{1}{16}\lambda^3 + \tfrac{1}{8}\lambda^5,$$

with $\lambda = (1+\delta)^{-1}$ the ratio of the sphere's radius to the distance of its centre from the wall, a result obtained by Keh & Anderson (1985) using reflection techniques. Keh & Anderson (1985) actually obtained a more accurate approximation, including an additional $O(\lambda^6)$ term. However, their analysis is based upon the implicit assumption that the particle is prevented from rotating. Therefore, only the $O(\lambda^3, \lambda^5)$ leading corrections, corresponding to the first wall reflection, are valid for the present case of a freely suspended particle. The second wall reflection, associated with the $O(\lambda^6)$ term, depends upon the sphere's angular velocity.

In order to understand the physical mechanism responsible for the velocity enhancement at small separations, it is necessary to consider the qualitative difference between electrophoresis and conventional Stokes-flow motion under an external field (e.g. gravity) in an electrolyte-free liquid. Since the linear Smoluchowski relation resembles the conventional mobility relation for a particle in Stokes flow, it can mistakenly be interpreted as representing a conventional force formula appropriate for an electrically charged body in the presence of an applied electric field. However, such an analogy is misleading, since the 'body' (which consists of a colloidal particle *and* its surrounding Debye layer) is electrically neutral. (Indeed, if the Debye screening length κ^{-1} is small compared with the linear particle dimension a, the zeta potential is actually $O(\kappa a)$ smaller (Probstein 1989) than the surface potential that a particle having the same surface charge would possess in an electrolyte-free liquid.) As explained by Anderson (1988), the mechanism underlying electrophoretic motion is that such a body is not rigid (owing to the relative fluid motion in the Debye layer). Thus, in contrast to the direct motion caused by an external field, electrophoresis results from indirect, ternary interactions between the external electric field, the particle, and the Debye layer.

In the case of remote boundary effects (Keh & Anderson 1985), such indirect interactions result in weak short-range forces that attenuate with the third power of the particle–wall distance (as opposed to the long-range forces resulting from wall effects in conventional Stokes flows, which are inversely proportional to this distance (Happel & Brenner 1965)). In the present analysis, however, the above-mentioned indirect interactions result in a different effect, which is related to the strong electric field existing in the gap region. This field exerts strong body forces on the non-neutral fluid elements comprising the Debye layer, thereby enhancing particle speed. (Obviously, this phenomenon has no counterpart in electrolyte-free externally driven motions.) While these body forces are explicitly absent from the bulk-scale description, they are nevertheless implicit in the large velocity slip prescribed at the particle surface.

As argued by Keh & Chen (1989), the interaction between the particle and the wall results in two oppositely directed effects. The first reflects the enhanced viscous retardation, acting to diminish the particle velocity. The second effect is the one discussed above, which is associated with intensification of the electric field in the gap region, acting to increase the particle velocity. (For $\delta \ll 1$, this field is $O(\delta^{\sqrt{2}/2-1})$.) While the former effect is dominant for particles that are relatively remote from the wall, the latter becomes comparable in magnitude to the former for small gap widths.

The present analysis is, of course, limited to the case where the gap width, while small compared with the particle dimension, is nevertheless large relative to the Debye-layer thickness. The investigation of the more general case, namely that of overlapping Debye layers, is a desirable extension of the present analysis. Such an investigation is probably possible within the framework of linear electrophoresis, and a similar one has been performed in the context of electrophoretic rotation of doublets (Velegol *et al.* 1998). It is important to note, however, that the Debye-layer thickness (which depends upon the equilibrium ionic concentration) may be of the order of nanometres for typical concentration values (Probstein 1989). Such small values suggest that the present model is likely to be valid for a wide range of gap widths.

A different limitation arises from the basic assumption underlying linear electrophoresis, namely a weak applied field. In the absence of wall effects it suffices to require that E_∞ be small compared with the natural scale of the electric field in the equilibrium Debye layer, namely $\kappa\zeta$. However, this requirement may not suffice in the present analysis, since the strong electric field existing in the gap region may invalidate the linear perturbation scheme about an equilibrium Debye-layer structure. Thus, it should be modified to the stronger form $\delta^{\sqrt{2}/2-1} \ll \kappa\zeta/E_\infty$. For typical values in encountered microfluidic devices (say, $\kappa \approx 10^9\,\mathrm{m}^{-1}$, $\zeta \approx 0.1\,\mathrm{V}$, and $E_\infty \approx 1000\,\mathrm{V\,m}^{-1}$) this asymptotic inequality extends over a wide range of (small) δ values.

Finally, we comment upon the potential use of the present mobility model. While it may appear from (6.8) that U and Ω both become unbounded as $\delta \to 0$, this trend is rendered invalid at gap separations of $O(\kappa^{-1})$, where the assumption of a thin Debye layer breaks down. However, since the divergence of the mobility as $\delta \to 0$ is rather weak (and, more importantly, integrable), it is expected that the local details of the thin Debye-layer region do not affect any integral results obtained using the present mobility data.† As such, the small-gap approximation for the mobility may be used when performing a macrotransport analysis entailing the electrokinetic motion of a Brownian particle in the presence of boundaries (cf. Brenner & Gaydos 1977). This will constitute the subject of a subsequent publication.

The authors are grateful to Eli Lilly and Company for their interest and financial support.

Appendix. The torque accompanying flow field (d)

The torque acting on the wall may be evaluated (at least to leading order) by using the respective asymptotic expressions for φ in the inner and outer regions. As the stresses on $\mathscr{W}$ do not give rise to any net force, this torque constitutes a couple. It is convenient to evaluate the pertinent force moments relative to the origin. In terms of cylindrical coordinates, this couple is given by the expression

$$\boldsymbol{T}_w = 2\gamma \int_0^{2\pi} \mathrm{d}\psi \int_0^{\infty} \mathrm{d}\rho\, \rho^2\, \boldsymbol{e}_\rho \times (\boldsymbol{e}_z \cdot \nabla\nabla\varphi)_{z=0}. \tag{A 1}$$

Introduction of the matching parameter, $\delta^{1/2} \ll \rho_0 \ll 1$, enables this integral to be separated into inner and outer contributions, corresponding to ρ-integration over the respective intervals $[0, \rho_0]$ and $[\rho_0, \infty]$. In terms of the appropriate coordinate systems, these contributions are respectively given by the expressions

$$\boldsymbol{T}_{w,\mathrm{inner}} = 2\gamma\delta^{1/2} \int_0^{2\pi} \mathrm{d}\psi \int_0^{\rho_0/\delta^{1/2}} \mathrm{d}R\, R^2 \boldsymbol{e}_\rho \times \left[\frac{\partial}{\partial Z}(\nabla\varphi)\right]_{Z=0}, \tag{A 2}$$

$$\boldsymbol{T}_{w,\mathrm{outer}} = 4\gamma \int_0^{2\pi} \mathrm{d}\psi \int_0^{2/\rho_0} \mathrm{d}\eta \frac{1}{\eta}\left[\boldsymbol{x} \times \frac{\partial}{\partial \xi}(\nabla\varphi)\right]_{\xi=0}. \tag{A 3}$$

Consider first the outer contribution. To leading order in δ we may let ρ_0 approach zero during the outer-region integration process. Use of (3.7) eventually yields

$$\boldsymbol{T}^{(0)}_{w,\mathrm{inner}} = 4\pi\gamma \mathscr{I}\, \boldsymbol{e}_y, \tag{A 4}$$

wherein

$$\mathscr{I} = \lim_{\eta_0\to\infty} \int_0^{\eta_0} \mathrm{d}\eta \left[\frac{M}{\eta} + 2\frac{\partial M}{\partial \eta} - \eta \frac{\partial^2 M}{\partial \xi^2}\right]_{\xi=0}. \tag{A 5}$$

Substitution into the above of (3.8), followed by interchange of the order of integration, yields

$$\mathscr{I} = \lim_{\eta_0\to\infty} \int_0^{\infty} \mathrm{d}s \frac{G(s)}{\sinh s} \int_0^{\eta_0} \mathrm{d}\eta \frac{J_1(s\eta)}{\eta} - \lim_{\eta_0\to\infty} \int_0^{\infty} \mathrm{d}s \frac{s^2 G(s)}{\sinh s} \int_0^{\eta_0} \mathrm{d}\eta\, \eta\, J_1(s\eta) \triangleq \mathscr{I}_1 - \mathscr{I}_2. \tag{A 6}$$

† This phenomenon resembles that for Prandtl's large-Reynolds-number boundary layer on a semi-infinite flat plate. The skin friction distribution obtained from the inner analysis is invalid near the leading edge. However, the weak divergence of that distribution near the edge allows evaluation of the leading-order drag on the plate without the need to separately analyse the leading-edge region (Van Dyke 1964).

In the evaluation of $\mathscr{I}_1$ the order of the limit process may be interchanged with the outer integration, so as to obtain

$$\mathscr{I}_1 = \int_0^\infty \mathrm{d}s \frac{G(s)}{\sinh s} \int_0^\infty \mathrm{d}\eta \frac{J_1(s\eta)}{\eta}. \tag{A 7}$$

The comparable calculation of $\mathscr{I}_2$ is not so straightforward, since the integral $\int_0^\infty \mathrm{d}\eta\, \eta\, J_1(s\eta)$ diverges. Instead, we first integrate the inner integral by parts to obtain

$$\mathscr{I}_2 = \lim_{\eta_0 \to \infty} \left[\int_0^\infty \mathrm{d}s \frac{sG(s)}{\sinh s} \int_0^{\eta_0} \mathrm{d}\eta\, J_0(s\eta) - \eta_0 J_0(s\eta_0) \int_0^\infty \mathrm{d}s \frac{sG(s)}{\sinh s} \right]. \tag{A 8}$$

It is permissible to interchange the order of the limit process and the inner integration in the first bracketed term. Use of the large-argument asymptotic expression for J_0 (Abramowitz & Stegun 1970) in the second term thereby yields, upon rearrangement,

$$\mathscr{I}_2 = \int_0^\infty \mathrm{d}s \frac{sG(s)}{\sinh s} \int_0^\infty \mathrm{d}\eta\, J_0(s\eta) - \lim_{\eta_0 \to \infty} \left(\frac{2\eta_0}{\pi} \right)^{1/2} \int_0^\infty \mathrm{d}s \frac{s^{1/2} G(s)}{\sinh s} \cos\left(s\eta_0 - \frac{\pi}{4} \right). \tag{A 9}$$

According to the Riemann–Lebesgue lemma, the last integral is attenuated as $O(1/\eta_0)$ for large η_0. Accordingly, the second term in (A 9) vanishes. Evaluation of the integrals of the Bessel functions (Gradshteyn & Rhyzhik 1980) yields

$$\mathscr{I}_1 = \mathscr{I}_2 = \int_0^\infty \mathrm{d}s\, \frac{G(s)}{\sinh s}. \tag{A 10}$$

Numerical integration gives $\mathscr{I} \approx -0.91$.

Next, consider the inner contribution to $\boldsymbol{T}_w$. From (3.37), (3.38) and (3.40) it is clear that

$$\left[\frac{\partial}{\partial Z} (\nabla\varphi) \right]_{Z=0} \sim \mu(\delta) \boldsymbol{e}_z \frac{R}{H^{(0)}(R)} \frac{\mathrm{d}G^{(0)}}{\mathrm{d}R} [1 + O(\delta)].$$

The integral (A 2) is obviously dominated by the large-R region, wherein the respective integrand diverges as $O(R^{\sqrt{2}-1})$. Thus, $\boldsymbol{T}_{w,\mathrm{inner}} \sim O(\rho_0^{\sqrt{2}}) \ll 1$. Hence, to leading order, $\boldsymbol{T}_w$ is given by the contribution of the outer region. This was to be expected, as the boundary conditions (d) do not introduce any singularity within the gap (as opposed, say, to the 'non-uniform' condition case (c)). A somewhat similar situation was observed by Jeffrey (1978) in the context of heat conduction, wherein the outer solutions became singular (as $\eta \to \infty$) only for 'non-uniform' (Dirichlet) boundary conditions (i.e. different temperatures on the wall and sphere).

We thus conclude that the wall experiences a finite couple, in contrast to that experienced by the sphere. Resolution of this apparent paradox concerns the non-uniformity of the far-field approximation (3.17) in the region near the wall, where $\xi \ll \eta$. Indeed, on the wall itself ($\xi = 0$) the main contribution to the integral representation (3.14) of M arises from the region $s \sim O(\eta^{-1})$. Use of the asymptotic form of G for large arguments yields, in terms of the integration variable $t = \eta s$,

$$M = \int_0^\infty \frac{G(s)}{\sinh s} J_1(\eta s)\, \mathrm{d}s \sim \frac{2}{\eta^2} \int_0^\infty t\, J_1(t)\, \mathrm{e}^{-2t/\eta}\, \mathrm{d}t. \tag{A 11}$$

Evaluation of this integral yields, when expressed in cylindrical coordinates,

$$\varphi^{(0)} \sim 4\frac{\cos\psi}{\rho}. \tag{A 12}$$

Thus, the effect of the plane is to diminish the rate of attenuation of the electro-osmotic velocity field at large distances from the sphere. Hence, any attempt to evaluate the torque on the sphere using Gauss's theorem is frustrated by the resulting slow attenuation, namely of $O(|\boldsymbol{x}|^{-3})$ for large $|\boldsymbol{x}|$, of the stresses near the wall.

REFERENCES

Abramowitz, M. & Stegun, I. A. 1970 *Handbook of Mathmatical Functions*. Dover.

Anderson, J. L. 1988 Colloid transport by interfacial forces. *Annu. Rev. Fluid Mech.* **30**, 139–165.

Batchelor, G. 1967 *An Introduction to Fluid Dynamics*. Cambridge University Press.

Böhmer, M. 1996 In situ observation of 2-dimensional clustering during electrophoretic deposition. *Langmuir* **12**, 5747–5750.

Brenner, H. 1964 The Stokes resistance of an arbitrary particle – IV. Arbitrary fields of flow. *Chem. Engng Sci.* **19**, 703–727.

Brenner, H. & Gaydos, L. J. 1977 The constrained Brownian movement of spherical particles in cylindrical pores of comparable radius: Models of the diffusive and convective transport of solute particles in membranes and porous media. *J. Colloid Interface Sci.* **58**, 312–356.

Cooley, M. D. A. & O'Neill, M. E. 1968 On the slow rotation of a sphere about a diameter parallel to a nearby plane wall. *J. Inst. Maths Applics.* **4**, 163–173.

Cox, R. G. 1997 Electroviscous forces on a charged particle suspended in a flowing liquid. *J. Fluid Mech.* **338**, 1–34.

Dean, W. R. & O'Neill, M. E. 1963 A slow motion of a viscous liquid caused by the rotation of a solid sphere. *Mathematika* **10**, 13–24.

Goldman, A. J., Cox, R. & Brenner, H. 1967*a* Slow viscous motion of a sphere parallel to a plane wall – I. Motion through a quiescent fluid. *Chem. Engng Sci.* **22**, 637–651.

Goldman, A. J., Cox, R. & Brenner, H. 1967*b* Slow viscous motion of a sphere parallel to a plane wall – II. Couette flow. *Chem. Engng Sci.* **22**, 663–660.

Gradshteyn, I. S. & Rhyzhik, I. M. 1980 *Table of Integrals, Series, and Products*. Academic.

Happel, J. & Brenner, H. 1965 *Low Reynolds Number Hydrodynamics*. Prentice-Hall.

Hu, H. H. & Joseph, D. D. 1999 Lift on a sphere near a plane wall in a second-order fluid. *J. Non-Newtonian Fluid Mech.* **88**, 173–184.

Jeffrey, D. J. 1978 The temperature field or electric potential around two almost touching spheres. *J. Inst. Maths Applics.* **22**, 337–351.

Jeffrey, D. J. & Chen, H. 1977 The virtual mass of a sphere moving towards a plane wall. *J. Appl. Mech.* **44**, 166–167.

Keh, H. J. & Anderson, J. L. 1985 Boundary effects on electrophoretic motion of colloidal spheres. *J. Fluid Mech.* **153**, 417–439.

Keh, H. J. & Chen, S. B. 1989 Electrophoresis of a colloidal sphere parallel to a dielectric plane. *J. Fluid Mech.* **194**, 377–390.

Latta, G. E. & Hess, G. 1973 Potential flow past a sphere tangent to a plane. *Phys. Fluids* **16**, 974–976.

Loewenberg, M. & Davis, R. H. 1993 Near-contact, thermocapillary migration of a nonconducting, viscous drop normal to a planar interface. *J. Colloid Interface Sci.* **160**, 265–274.

Miloh, T. 1977 Hydrodynamics of deformable contiguous spherical shapes in an incompressible inviscid fluid. *J. Engng Maths* **11**, 349–372.

Moon, P. & Spencer, D. E. 1988 *Field Theory Handbook*. Springer.

Morrison, F. A. 1970 Electrophoresis of a particle of arbitrary shape. *J. Colloid Interface Sci.* **34**, 210–214.

O'Brien, R. W. 1983 The solution of the electrokinetic equations for colloidal particles with thin double layers. *J. Colloid Interface Sci.* **92**, 204–216.

O'Brien, R. W. & Hunter, R. J. 1981 The electrophoretic mobility of large colloidal particles. *Can. J. Chem.* **59**, 1878–1887.

O'Brien, R. W. & White, L. R. 1978 Electrophoretic mobility of a spherical colloidal particle. *J. Chem. Soc. Faraday* II **74**, 1607–1626.

O'Neill, M. E. 1964 A slow motion of a viscous liquid caused by a slowly moving solid sphere. *Mathematika* **11**, 64–74.

O'Neill, M. E. & Stewartson, K. 1967 On the slow motion of a sphere parallel to a nearby plane wall. *J. Fluid Mech.* **27**, 705–724.

Paley, A. V., Radchik, A. & Smith, G. B. 1993 Quasistatic optical response of pairs of touching spheres with arbitrary dielectric permeability. *J. Appl. Phys.* **73**, 3446–3453.

Probstein, R. F. 1989 *Physicochemical Hydrodynamics*. Butterworths.

Russel, W. B., Saville, D. A. & Schowalter, W. R. 1989 *Colloidal Dispersions*. Cambridge University Press.

Sneddon, I. N. 1972 *The Use of Integral Transforms*. McGraw-Hill.

Solomentsev, Y., Velegol, D. & Anderson, J. L. 1997 Conduction in the small gap between two spheres. *Phys. Fluids* **9**, 1209–1217.

Stone, H. A. & Kim, S. 2001 Microfluidics: basic issues, applications, and challenges. *AIChE J.* **47**, 1250–1254.

Teubner, M. 1982 Motion of charged colloidal particles in electric fields. *J. Chem. Phys.* **76**, 5564–5573.

Van Dyke, M. 1964 *Perturbation Methods in Fluid Mechanics.* Academic.

Velegol, D., Solomentsev, Y., Anderson, J. L. & Carnie, S. L. 1998 Electrophoretic rotation of doublets composed of two spheres almost in contact. *Colloid Surf.* A **140**, 59–74.

Warszyński, P., Wu, X. & van de Ven, T. G. M. 1998 Electrokinetic lift force for a charged particle moving near a charged wall – a modified theory and experiment. *Colloid Surf.* A **140**, 183–198.

Yariv, E. & Brenner, H. 2003 The electrophoretic mobility of a closely-fitting sphere in a cylindrical pore. *SIAM J. App. Maths* (to appear).

Zeng, S., Zinchenko, A. Z. & Davis, R. H. 1999 Electrophoretic motion of two interacting particles. *J. Colloid Interface Sci.* **209**, 282–301.